Aalto University
School of Science

Two topics beyond perfect crystals: quantum geometry of evanescent surface states in rhombohedral graphite, and topological charges in quasicrystals

Päivi Törmä

Aalto University

Topology and Geometry Beyond Perfect Crystals, Nordita, Stockholm, Sweden

11.6.2025

Super C Room Temperature Superconductivity 2033

Institute Q

ACADEMY OF FINLAND

Contents

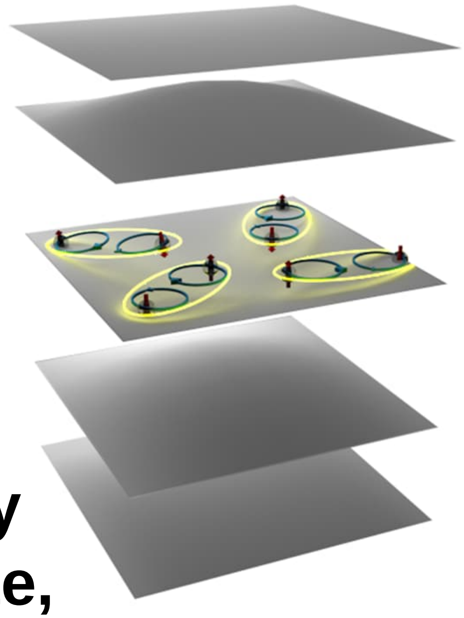

Quantum geometry and superconductivity

Lowest-Landau-level (LLL) quantum geometry of the surface states of rhombohedral graphite, and superconductivity

High topological charge lasing in a quasicrystal

Contents

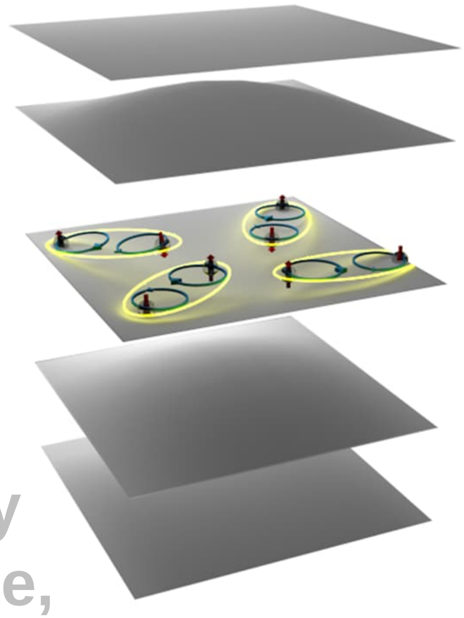

Quantum geometry and superconductivity

Lowest-Landau-level (LLL) quantum geometry of the surface states of rhombohedral graphite, and superconductivity

High topological charge lasing in a quasicrystal

Quantum geometric tensor

Metric for the distance between quantum states

Provost, Vallee, Comm. Math. Phys. **76**, 289 (1980)

$$d\ell^2 = ||u(\mathbf{k}+d\mathbf{k}) - u(\mathbf{k})||^2 = \langle u(\mathbf{k}+d\mathbf{k}) - u(\mathbf{k})|u(\mathbf{k}+d\mathbf{k}) - u(\mathbf{k})\rangle$$

$$\approx \sum_{i,j} \underbrace{\langle \partial_{k_i} u|\partial_{k_j} u\rangle}\, dk_i dk_j$$

Introduce gauge invariant version $\left(u(\mathbf{k}) \leftrightarrow u(\mathbf{k})e^{i\phi(\mathbf{k})}\right)$

➡ Quantum geometric tensor (Fubini-Study metric)

$$\mathcal{B}_{ij}(\mathbf{k}) = 2\langle \partial_{k_i} u|(1 - |u\rangle\langle u|)|\partial_{k_j} u\rangle$$

$\mathrm{Re}\,\mathcal{B}_{ij} = g_{ij}$ quantum metric $d\ell^2 = \sum_{ij} g_{ij} dk_i dk_j$

$\mathrm{Im}\,\mathcal{B}_{ij} = [\mathbf{\Omega}_{\mathrm{Berry}}]_{ij}$ Berry curvature

Chern number: $C = \dfrac{1}{2\pi}\displaystyle\int_{\mathrm{B.Z.}} \mathrm{d}^2\mathbf{k}\, \Omega_{\mathrm{Berry}}(\mathbf{k})$

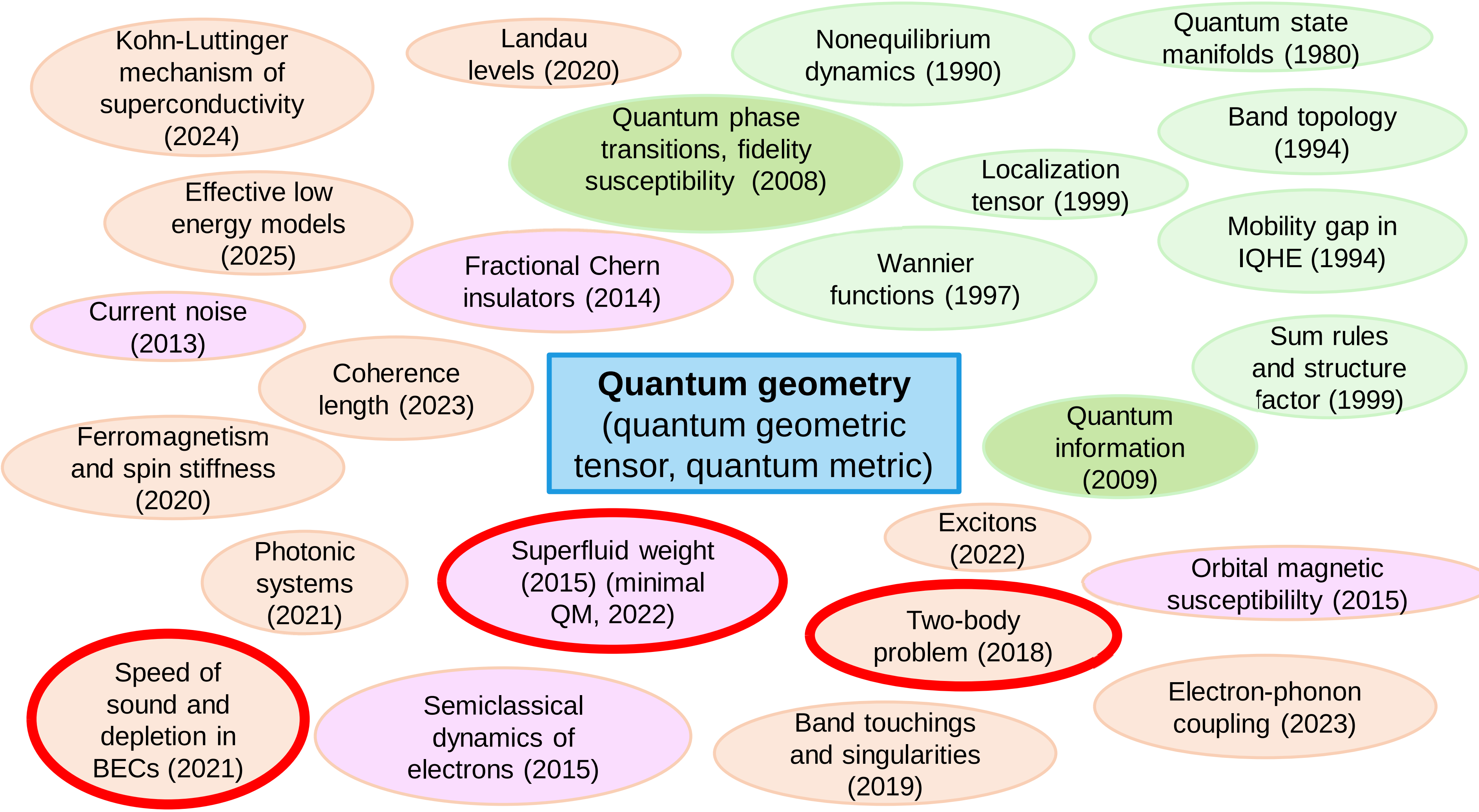

Perspective on quantum geometry
PT, PRL 2023
Review on quantum geometry
Yu, Bernevig, Queiroz, Rossi, PT, Yang, arXiv 2025

Review on quantum geometric superconductivity
PT, Peotta, Bernevig, Nat. Rev. Phys. 2022

Superconductivity: Cooper pair formation competes with kinetic energy

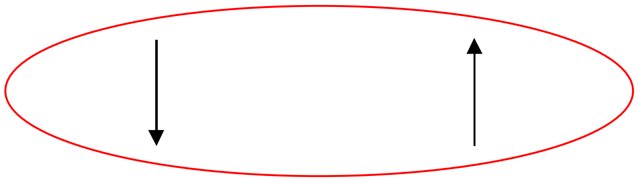

Weak interaction U
Large kinetic energy (Fermi level)
Low critical temperature

$$T_c \propto e^{-1/(U n_0(E_f))}$$

Constituents: interactions, density of states (DOS)

Remove the kinetic energy/maximize DOS: interaction effects dominate!

Flat bands: interactions dominate

Dispersive band U<<W:

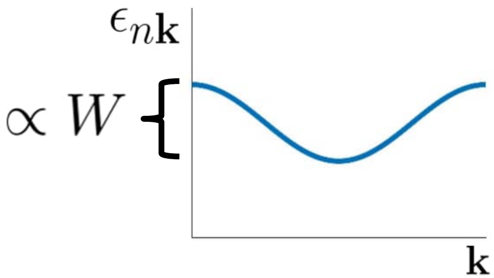

$$\psi_n(\mathbf{r}) = e^{i\mathbf{k}\cdot\mathbf{r}} u_{n\mathbf{k}}(\mathbf{r})$$

(periodic part of) the Bloch function

T_c for Cooper pairing

$$T_c \propto e^{-1/(U n_0(E_f))}$$

Flat band U>>W:

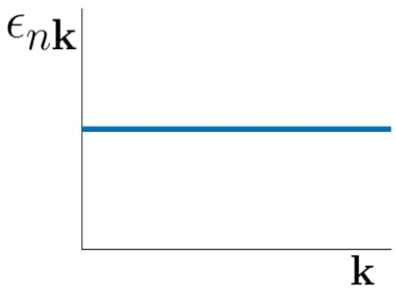

$\epsilon_{n\mathbf{k}} =$ constant

Group velocity: $\frac{\partial \epsilon_{n\mathbf{k}}}{\partial k} = 0$

No interactions: insulator at any filling

$$T_c \propto U V_{\text{flat band}}$$

High T_c for pairing
(Khodel, Shaginyan, Volovik, Kopnin, Heikkilä)

This is the critical temperature for Cooper pairing

$$\Delta(\mathbf{r}) = \langle \psi_\sigma(\mathbf{r}) \psi_{\sigma'}(\mathbf{r}) \rangle \qquad \Delta(\mathbf{r}) = |\Delta(\mathbf{r})|$$

Superfluid weight: supercurrent and Meissner Effect

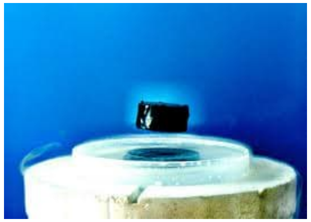

Supercurrent

$$\mathbf{j} = -D_s \mathbf{A}$$

Current

$$\mathbf{j} = \sigma \mathbf{E} \qquad \mathbf{E} = -\partial \mathbf{A}/\partial t$$

Order parameter phase gradient $\quad \Delta(\mathbf{r}) = |\Delta(\mathbf{r})| \mathrm{e}^{2i\phi(\mathbf{r})}$

$\nabla\phi - e\mathbf{A}/\hbar$ Invariant under gauge transformations

Free energy change associated with phase gradient

$$\Delta F = \frac{\hbar^2}{2e^2} \int \mathrm{d}^3\mathbf{r} \sum_{ij} [D_s]_{ij} \partial_i \phi(\mathbf{r}) \partial_j \phi(\mathbf{r})$$

London equation and penetration depth

$$\nabla \times \mathbf{B} = \mu_0 \mathbf{j}$$

$$\nabla^2 \mathbf{B} = \mu_0 D_s \mathbf{B}$$

$$\lambda_L = (\mu_0 D_s)^{-1/2}$$

Superfluid weight: supercurrent and Meissner Effect

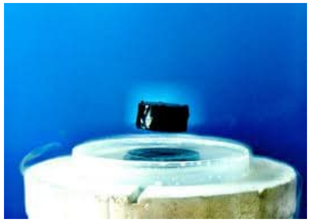

Supercurrent

$$\mathbf{j} = -D_s \mathbf{A}$$

Current

$$\mathbf{j} = \sigma \mathbf{E} \qquad \mathbf{E} = -\partial \mathbf{A}/\partial t$$

Order parameter phase gradient $\quad \Delta(\mathbf{r}) = |\Delta(\mathbf{r})| \mathrm{e}^{2i\phi(\mathbf{r})}$

$\nabla \phi - e\mathbf{A}/\hbar$ Invariant under gauge transformations

Free energy change associated with phase gradient

$$\Delta F = \frac{\hbar^2}{2e^2} \int \mathrm{d}^3\mathbf{r} \sum_{ij} [D_s]_{ij} \partial_i \phi(\mathbf{r}) \partial_j \phi(\mathbf{r})$$

Conventional BCS: $D_s = \frac{e^2 n_\mathrm{p}}{m_\mathrm{eff}} \left(1 - \left(\frac{2\pi\Delta}{k_\mathrm{B}T} \right)^{1/2} \mathrm{e}^{-\Delta/(k_\mathrm{B}T)} \right)$

Zero at a flat band!!!

n_p Particle density

$\frac{1}{m_\mathrm{eff}} \propto J \propto \partial_{k_i} \partial_{k_j} \epsilon_\mathbf{k}$ Bandwidth $\qquad i, j = x, y, z$

Formation of flat bands

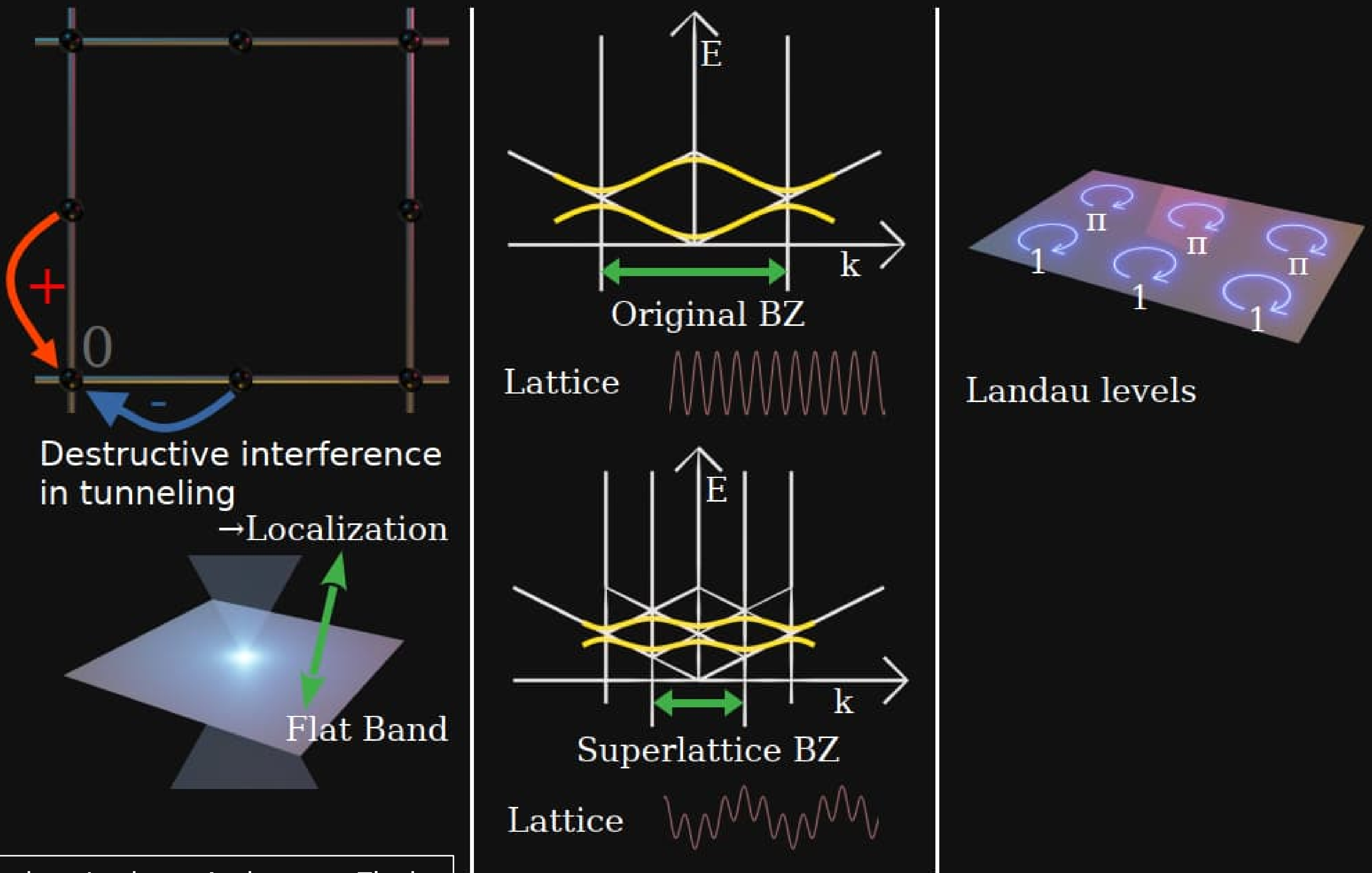

Review: Leykam, Andreanov, Flach, Advances in Physics 2018

Superfluidity and quantum geometry

Sebastiano Peotta

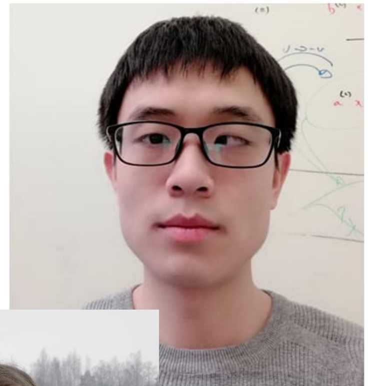

Long Liang

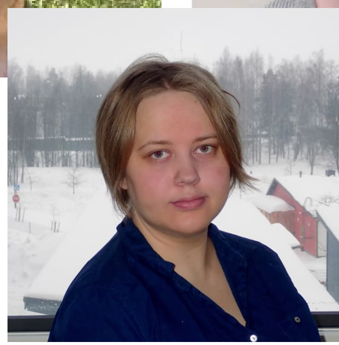

Kukka-Emilia Huhtinen

Andrei Bernevig

Sebastian Huber

Murad Tovmasyan

Jonah Herzog-Arbeitman

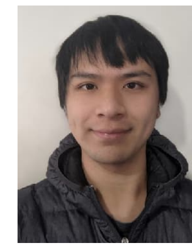

Aaron Chew

Aleksi Julku

Dong-Hee Kim

Tuomas Vanhala

Ari Harju

Topi Siro

Peotta, PT, Nat Comm 2015
Julku, Peotta, Vanhala, Kim, PT, PRL 2016
Tovmasyan, Peotta, PT, Huber, PRB 2016
Liang, Vanhala, Peotta, Siro, Harju, PT, PRB 2017
Liang, Peotta, Harju, PT, PRB 2017
Tovmasyan, Peotta, Liang, PT, Huber, PRB 2018
PT, Liang, Peotta, PRB(R) 2018
Huhtinen, Herzog-Arbeitman, Chew, Bernevig, PT, PRB 2022
Herzog-Arbeitman, Chew, Huhtinen, PT, Bernevig, arXiv 2022

Our multiband approach

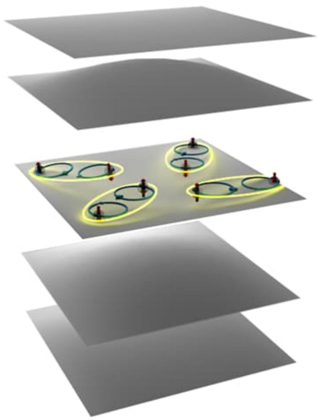

MULTIBAND BCS MEAN-FIELD THEORY
multiband two-component attractive
Fermi-Hubbard model –U < 0

$$H = -\sum_{ij\alpha\beta\sigma} t^{\sigma}_{i\alpha j\beta} c^{\dagger}_{i\alpha\sigma} c_{j\beta\sigma} - U \sum_{i\alpha} n_{i\alpha\uparrow} n_{i\alpha\downarrow} - \mu \sum_{i\alpha\sigma} n_{i\alpha\sigma}$$

Introduce supercurrent

$$\Delta(\mathbf{r}) \rightarrow \Delta(\mathbf{r}) e^{2i\mathbf{q}\cdot\mathbf{r}}$$

$$\nabla\phi - e\mathbf{A}/\hbar$$

$2\mathbf{q}$ Cooper pair momentum

$$\langle j_i(\omega, \mathbf{q})\rangle = -\sum_j \chi_{ij}(\omega, \mathbf{q}) A_j(\omega, \mathbf{q})$$

$$[D_s]_{ij} = \frac{e^2}{V} \frac{d^2 E}{dq_i dq_j}\Big|_{\mathbf{q}=0}$$

$$D_s = \lim_{\mathbf{q}\rightarrow 0} \chi(\omega = 0, \mathbf{q})$$

$i, j = x, y, z$

Superfluid weight in a multiband system

$$D_s = D_{s,\mathrm{conventional}} + D_{s,\mathrm{geometric}}$$

$$i, j = x, y, z$$

$$\propto \partial_{k_i} \partial_{k_j} \epsilon_{\mathbf{k}}$$

Can be nonzero also in a flat band
Present only in a multiband case
Proportional to the quantum metric

$$[D_{s,\mathrm{geometric}}]_{ij} \propto U g_{ij}$$

Lower bound for flat band superfluidity

Peotta, PT, Nat Comm 2015

The quantum geometric tensor $\mathcal{B}_{ij}$
is complex positive semidefinite

$$\Rightarrow \boxed{D_s \geqslant \int_{B.Z.} d^d\mathbf{k} |\mathbf{\Omega}_{\mathrm{Berry}}(\mathbf{k})| \geqslant C}$$

Time reversal symmetry assumed; C is a spin Chern number

Constituents: interactions, density of states (DOS)
and Bloch functions = quantum geometry and topology

Why can there be transport in a flat band?

Localization and flat band due to vanishing overlap

Localization and flat band due to interference

Non-interacting

Interacting

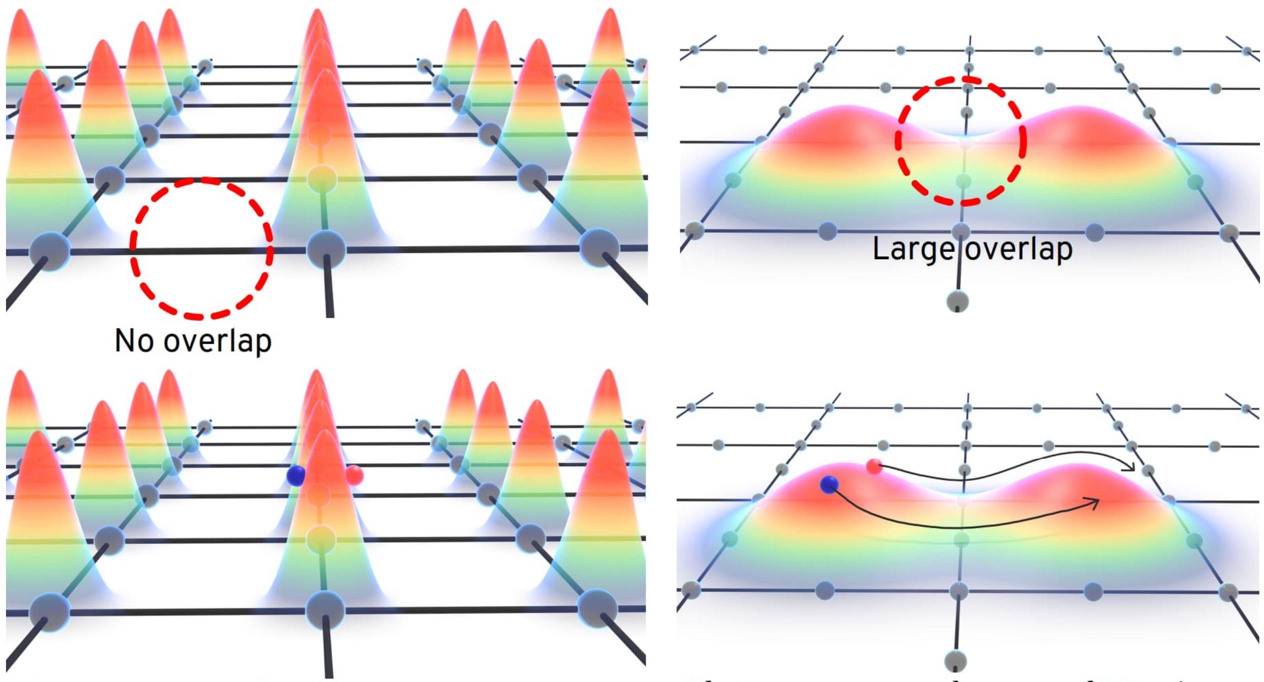

Electrons stay localized

Electrons can move because of Wannier function overlap

$$C \neq 0 \Leftrightarrow \text{non-localized } w(\mathbf{r}) = \mathcal{F}[u(\mathbf{k})]$$

Brouder, Panati, Calandra, Marzari, PRL 2007

$$D_s \propto g_{ij} \geqslant C$$

Twisted Bilayer Graphene (TBG) superconductivity since 2018

Reviews: Balents, Dean, Efetov, Young, Nat Phys 2020

Andrei, Efetov, Jarillo-Herrero, MacDonald, Mak, Senthil, Tutuc, Yazdani, Young, Nat Rev Mater 2021

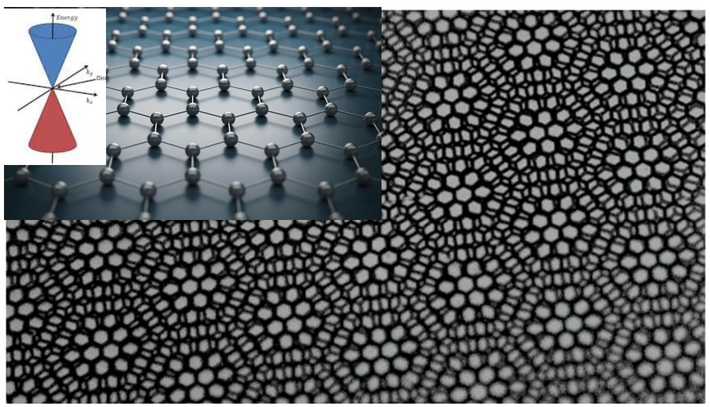

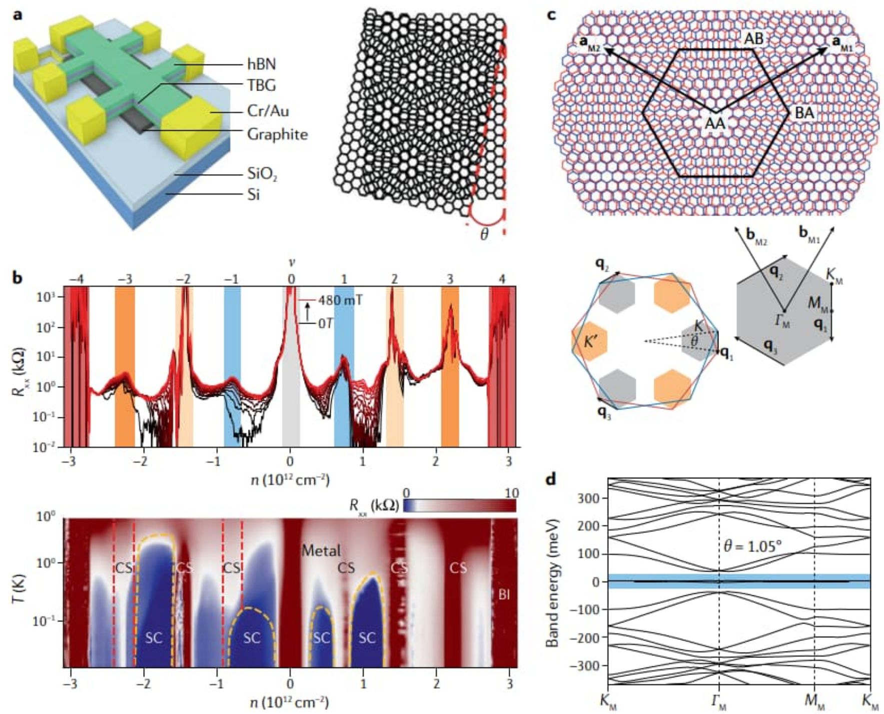

Figure credits see Fig.1 in

PT, Peotta, Bernevig, Nat Rev Phys 2022

Quantum geometry: Relevant for TBG superconductivity?

Theoretically suggested:
Julku, Peltonen, Liang, Heikkilä, PT, PRB 2020
Hu, Hyart, Pikulin, Rossi, PRL 2020
Xie, Song, Lian, Bernevig PRL2020

Tian,… , Randeria, Lau, Bockrath, Nature 2023

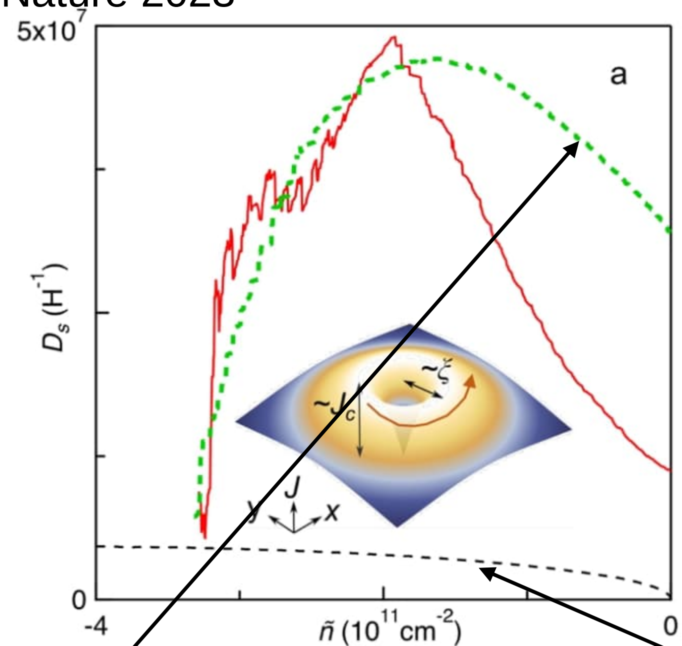

Tanaka,…, Jarillo-Herrero, Oliver, Nature 2025

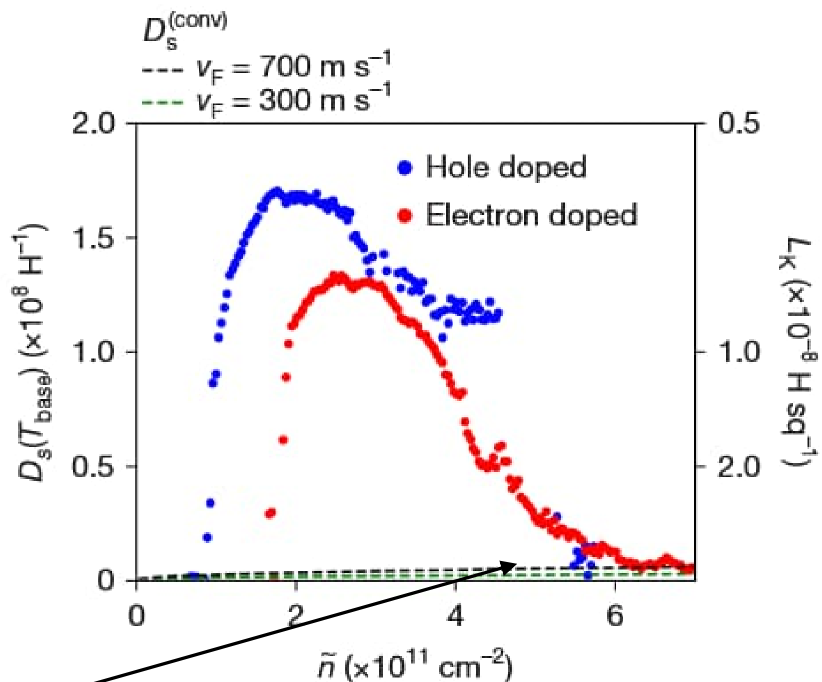

$$D_s(0,\tilde{n}) \approx b\frac{e^2}{\hbar^2}\Delta(0,\tilde{n})$$

$$D_s(T) = \frac{e^2 n_s(T)}{m}$$

Isolated flat band
Peotta, PT, Nat Comm 2015

$$[D_s]_{ij} = \frac{2}{\pi\hbar^2}\frac{\Delta^2}{UN_{\mathrm{orb}}}\mathcal{M}_{ij}^{\mathrm{R}}$$

Contents

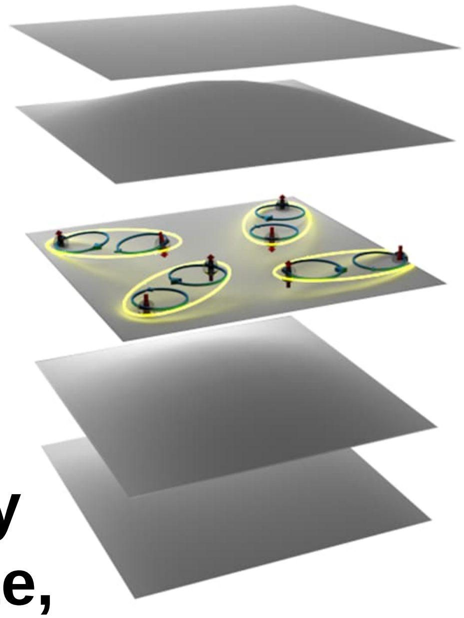

Quantum geometry and superconductivity

Lowest-Landau-level (LLL) quantum geometry of the surface states of rhombohedral graphite, and superconductivity

High topological charge lasing in a quasicrystal

Quantum geometry of the surface states of rhombohedral graphite and its effects on the surface superconductivity

Guodong Jiang

Tero Heikkilä

Jiang, Heikkilä, PT, arXiv:2504.03617 (2025)

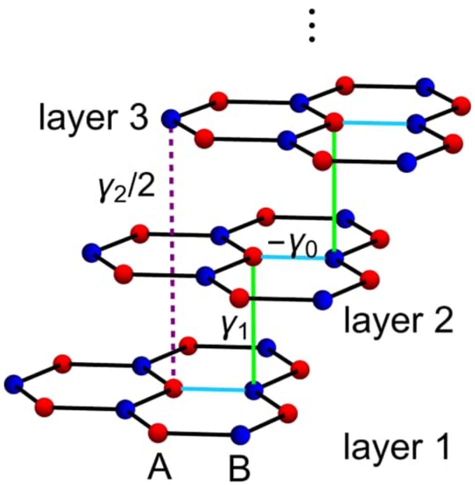

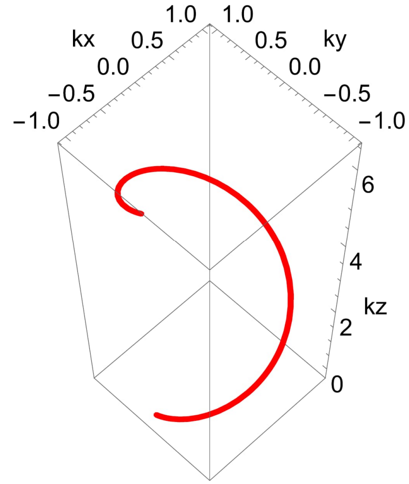

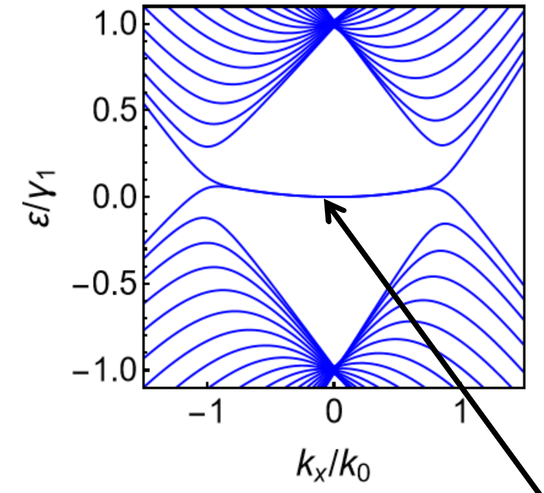

Drumhead surface states

$$\hat{H} = \{-\gamma_0 \sum_{n,\langle iA,jB\rangle} c^{+}_{niA} c_{njB} + \gamma_1 \sum_{n} c^{+}_{n+1,iA} c_{niB}\} + h.c.$$

F. T. $$h(k_x, k_y, k_z) = \begin{pmatrix} 0 & c.c. \\ k_x + ik_y + e^{ik_z} & 0 \end{pmatrix}$$

In scaled units: γ_1 (energy), γ_0/v_f (momentum).

Degeneracies:

$$k_x + ik_y + e^{ik_z} = 0 \Longrightarrow \begin{cases} k_x = -\cos k_z \\ k_y = -\sin k_z \end{cases}$$ nodal spiral

Two incomplete pictures of RG surface states:

(1) Su-Schrieffer-Heeger model

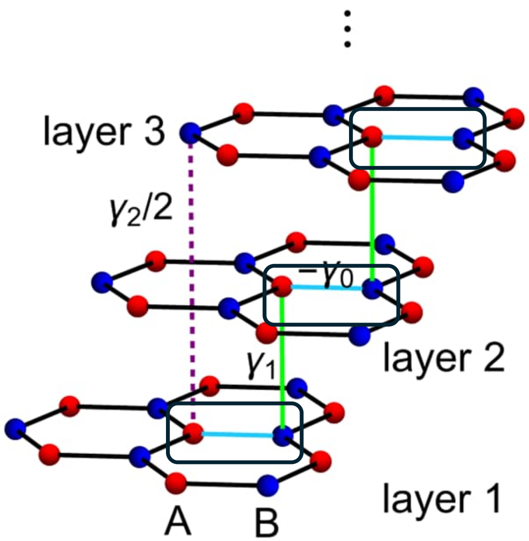

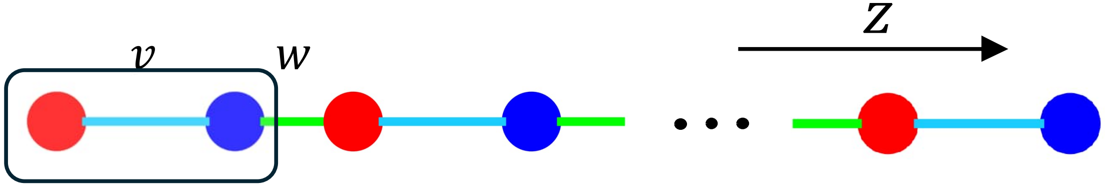

$|w| > |v|$: topological phase, two E=0 edge states

$$h(k_z) = \begin{pmatrix} 0 & c.c. \\ v + we^{ik_z} & 0 \end{pmatrix}$$

SSH model corresponds to only one point $(k_x, k_y) = (\frac{v}{w}, 0)$ in the drumhead region.

For RG, surface state decay length varies with $\mathbf{k}$!

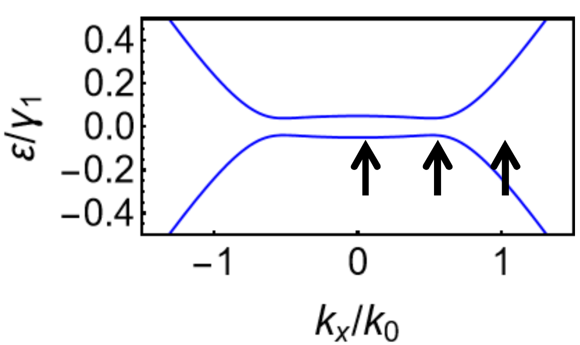

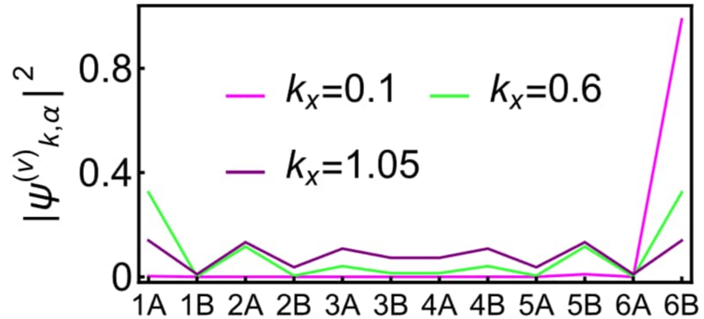

(2) Two-orbital effective model

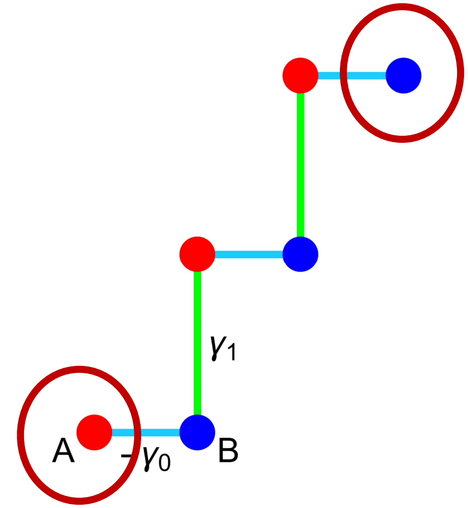

From perturbation theory ($H = H_0 + H'$)

$$H_{\text{eff}} = E_0 + P_0 H' \sum_{j=1}^{\infty} (\tilde{G}_0 H')^j P_0 \, ,$$

$$P_0 = \begin{pmatrix} 1 & & & \\ & 0 & & \\ & & \ddots & \\ & & & 1 \end{pmatrix}$$ is the projection to 1A and NB,

$$\tilde{G}_0 = P_1 \frac{1}{E_0 - H_0} P_1, \, P_1 = 1 - P_0 \qquad \Longrightarrow \qquad H_{\text{eff}} = (-1)^{N-1} \begin{pmatrix} m & \pi^{*N} \\ \pi^N & -m \end{pmatrix}$$

$$\pi = k_x + i k_y$$ McCann 2006, Guinea 2006, Min 2008, etc.

limitations:

- **good dispersion near the center**
- **good quantum geometry at the rim**
- **topologically incorrect**

Quantum metric of RG surface states

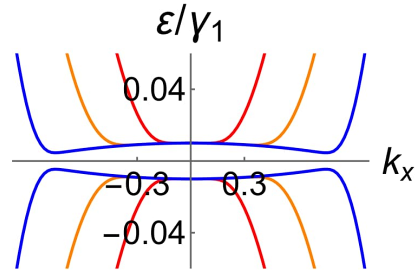

Dispersion with small surface potential

Tight binding (✓) VS Two-orbital effective (✗)

$m = 0.01\gamma_1$

Increase surface potential m

$m = 0.1\gamma_1$

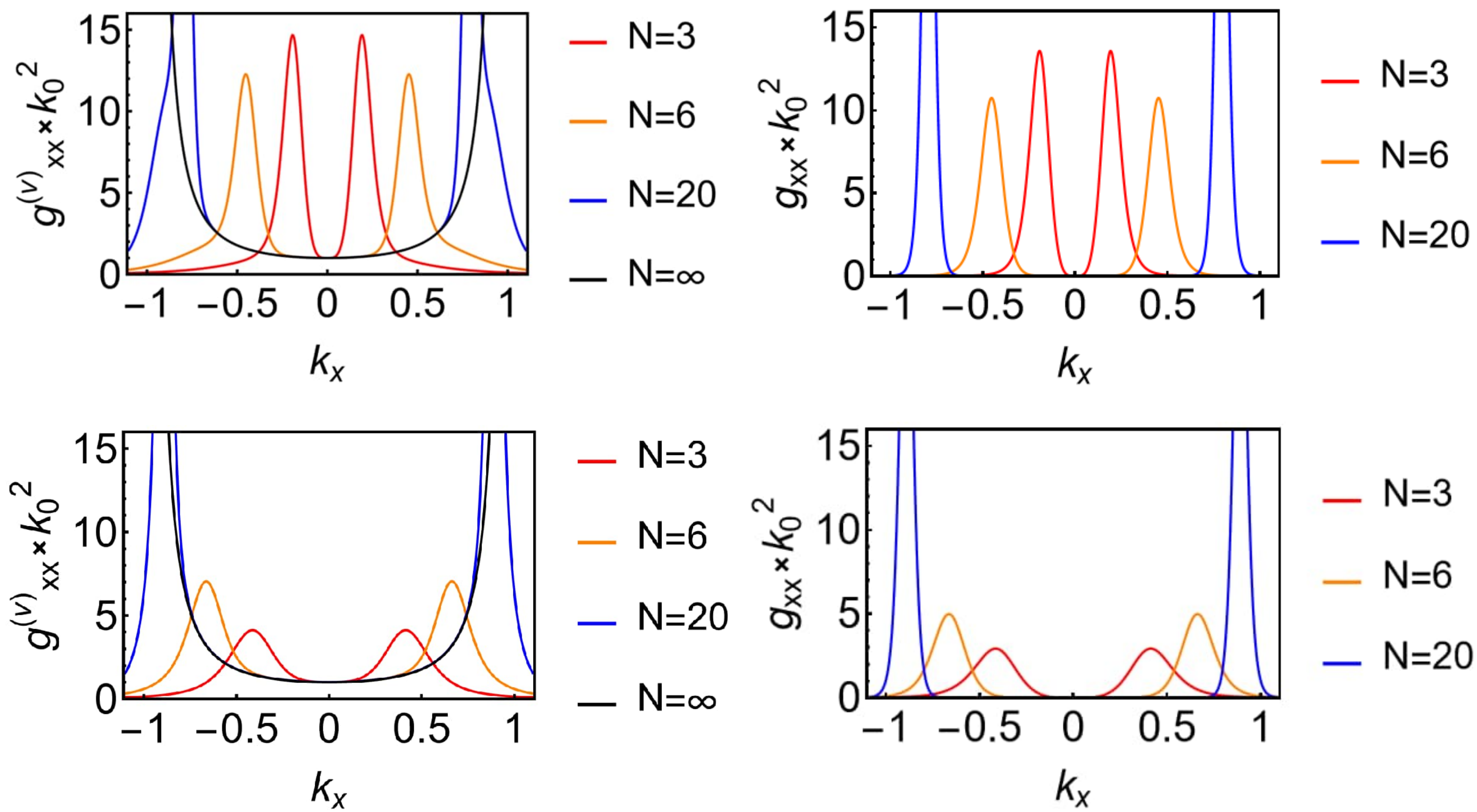

v: valence band

QGT of RG surface states

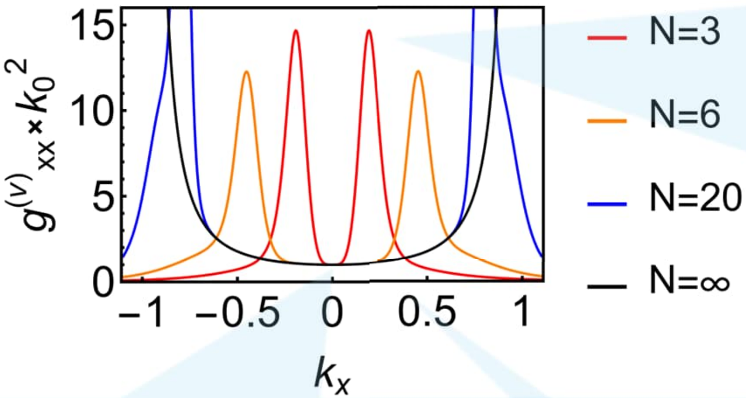

(1) Nonzero at the center

N=∞ limit:

$$\psi_{\mathbf{k}}^{(v)}(z) = \frac{\sqrt{1-k^2}}{k} e^{\kappa(\mathbf{k})z} \begin{pmatrix} 1 \\ 0 \end{pmatrix}$$

$$\kappa(\mathbf{k}) = \ln[-(k_x + ik_y)]$$

QGT $B_{\mu\nu}^{(v)}(\mathbf{k}) = \frac{1}{(1-k^2)^2} \begin{pmatrix} 1 & i \\ -i & 1 \end{pmatrix}$

The nonzero value is from the **momentum-dependent decay, i.e.** $\nabla_{\mathbf{k}}\kappa$

(2) Peak at the rim

A surface hybridization effect. At some momentum, $\lambda(\mathbf{k}) = 1/\kappa(\mathbf{k}) \sim$ N.

$$B_{\mu\nu}^{(v)}(\mathbf{k}) \equiv \sum_l \langle \partial_\mu \psi_{\mathbf{k}}^{(v)} | \psi_{\mathbf{k}}^{(l)} \rangle \langle \psi_{\mathbf{k}}^{(l)} | \partial_\nu \psi_{\mathbf{k}}^{(v)} \rangle$$

Focus on the $l = c$ term

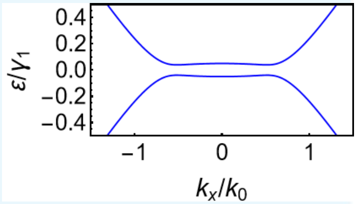

$$\Longrightarrow \frac{\langle \psi_{\mathbf{k}}^{(v)} | \partial_\mu H_{\mathbf{k}} | \psi_{\mathbf{k}}^{(c)} \rangle \langle \psi_{\mathbf{k}}^{(c)} | \partial_\nu H_{\mathbf{k}} | \psi_{\mathbf{k}}^{(v)} \rangle}{\left(\varepsilon_{v,\mathbf{k}} - \varepsilon_{c,\mathbf{k}}\right)^2}$$

Jiang, Heikkilä, PT, arXiv: 2504.03617
Bernevig, Kwan, arXiv: 2503.09692
(Different approaches)

(3) N-independent at the center

No surface hybridization
$\Longrightarrow$ wavefunctions for different N are the same.

LLL quantum geometry

$$B = g - \frac{i}{2}\Omega, \qquad \mathrm{Tr}[g] \geq |\Omega|$$

$$B_{\mu\nu}^{(v/c)}(\mathbf{k}) = \frac{1}{(1-k^2)^2}\begin{pmatrix} 1 & \pm i \\ \mp i & 1 \end{pmatrix}$$ Quantum geometric tensor of RG

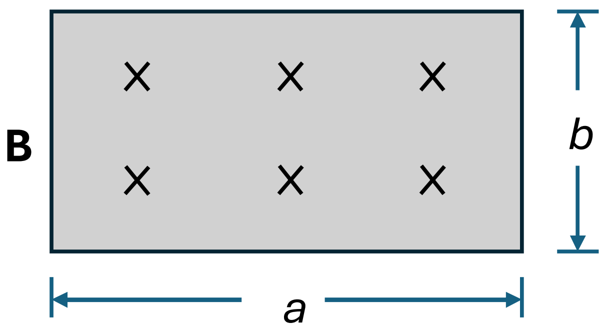

A fictitious unit cell

Hamiltonian of the LL problem:

$$H = \frac{(\mathbf{p} + \mathbf{A})^2}{2m}, \qquad (e = \hbar = 1)$$

Quantum geometric tensor of LL

$$B_{\mu\nu}^{n}(\mathbf{k}) = \frac{l_B^2}{2}\begin{pmatrix} 2n+1 & -i \\ i & 2n+1 \end{pmatrix}, \quad n = 0, 1, \ldots$$

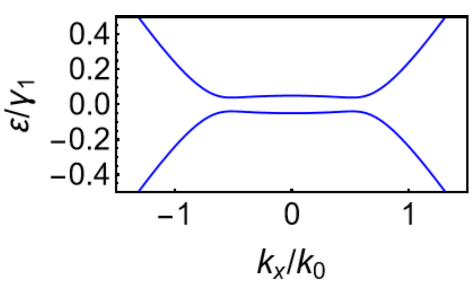

The two surface bands of RG resemble a pair of decoupled LLLs with opposite B fields

Superconductivity and surface polarization

Effects of long-range hoppings:

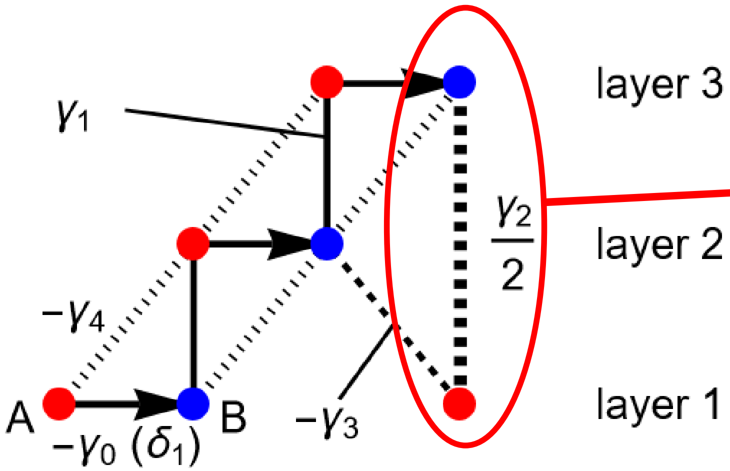

Dispersion at m=0:

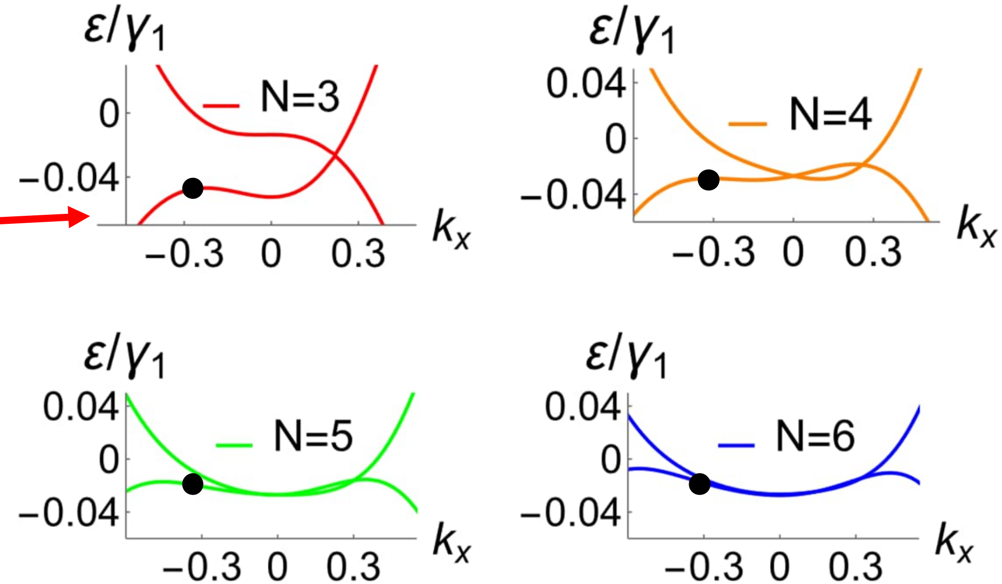

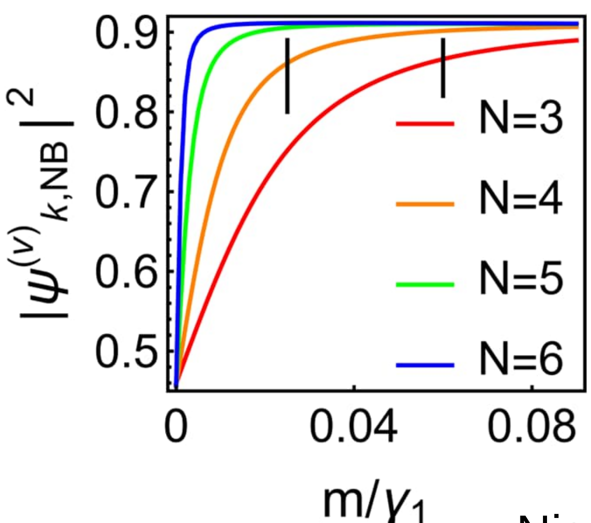

Displacement field has two effects:
(1) Flatten the band and enhance DOS;
(2) Polarize electron density to one surface

Once m is above the m_s, QGT is the same as previously discussed !

Nissinen, Heikkilä, Volovik (2021) PRB 103, 245115

Superconductivity and surface polarization

Gap equation in orbital basis (onsite pairing, s-wave and doped to the valence band)

$$\Delta_\alpha = -U\langle c_{i\alpha\downarrow} c_{i\alpha\uparrow}\rangle \qquad \alpha\text{=1A or NB}$$

$$\Delta_v(k) = \left|\psi^{(v)}_{k,1A}\right|^2 \Delta_{1A} + \left|\psi^{(v)}_{k,NB}\right|^2 \Delta_{NB}$$

At full polarization, **effective coupling strength for one order (e.g. Δ_{NB}) is doubled**.

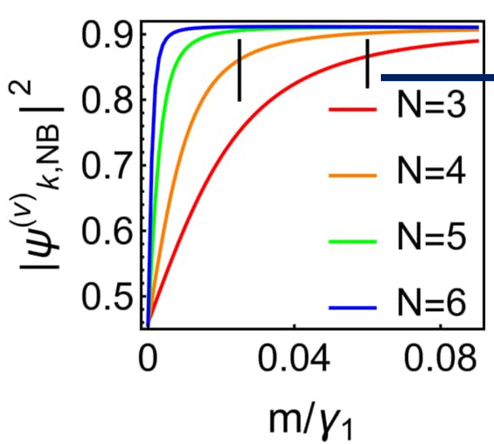

m_s of trilayer ~23 meV

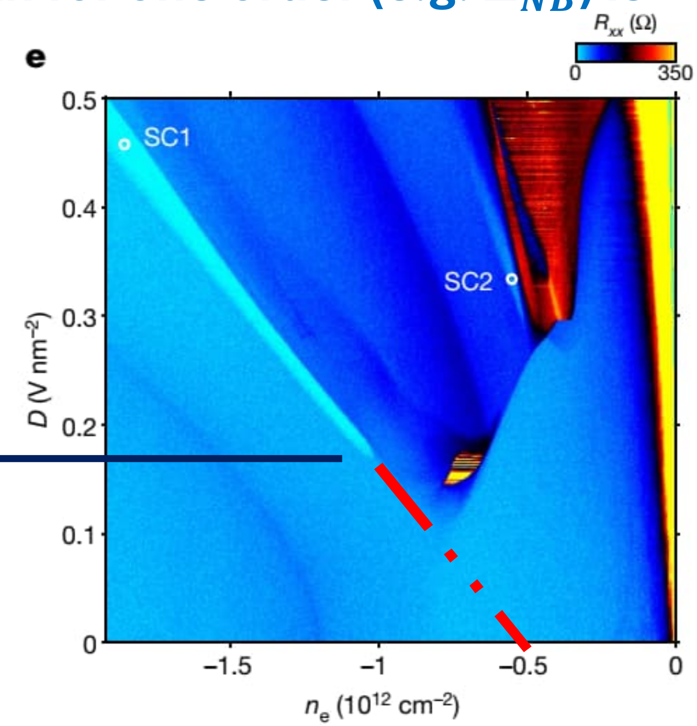

Zhou… Young, Nature 2021

Superconductivity and topological heavy-fermion model

Fictitious superconducting state in large N-layer RG:

Distribution of superfluid stiffness in **k**-space:

$$D_{s,\mu\nu} = 2\sum_{\mathbf{k}}[f_{\mu\nu}^{\mathrm{conv}}(\mathbf{k}) + f_{\mu\nu}^{\mathrm{geo}}(\mathbf{k})]$$

dispersion

$$f_{\mu\nu}^{\mathrm{conv}}(\mathbf{k}) = -\left(\frac{\xi_{v,\mathbf{k}}}{E_{v,\mathbf{k}}} + 1\right)\partial_\mu\partial_\nu\xi_{v,\mathbf{k}}$$

Pairing matrix in orbital basis

$$f_{\mu\nu}^{\mathrm{geo}}(\mathbf{k}) = \frac{1}{E_{v,\mathbf{k}}}\mathrm{Tr}\{\partial_\mu P_{\mathbf{k}}^{(v)}\hat{\Delta}\partial_\nu P_{\mathbf{k}}^{(v)}\hat{\Delta} - \partial_\mu\partial_\nu P_{\mathbf{k}}^{(v)}\hat{\Delta}P_{\mathbf{k}}^{(v)}\hat{\Delta}\}$$

Fully polarized order parameter:

$$\hat{\Delta} = \begin{pmatrix} 0 & & & \\ & \ddots & & \\ & & 0 & \\ & & & \Delta_{NB} \end{pmatrix}$$

$$f_{\mu\nu}^{\mathrm{geo}}(\mathbf{k}) = 2\Delta_{NB}(\delta_{\mu\nu} + \frac{2}{1-k^2}k_\mu k_\nu)$$

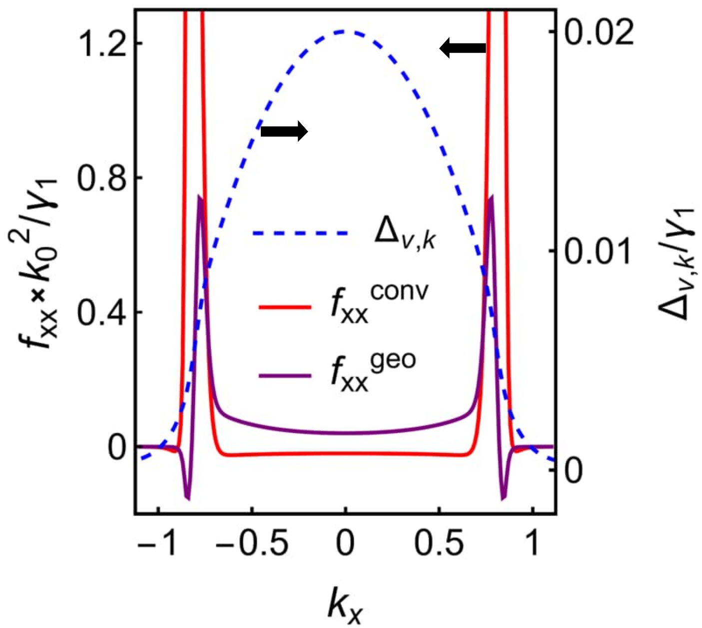

Superconductivity and topological heavy-fermion model

Unusual heavy-fermion picture of RG

Usual topological HF (Song, Bernevig, PRL 2022)
f-electron localized in all dimensions;
Wannierizable;

We find: Unusual RG HF
only localized in z direction, and delocalized in x-y direction (LLL QG);
non-Wannierizable (topological)

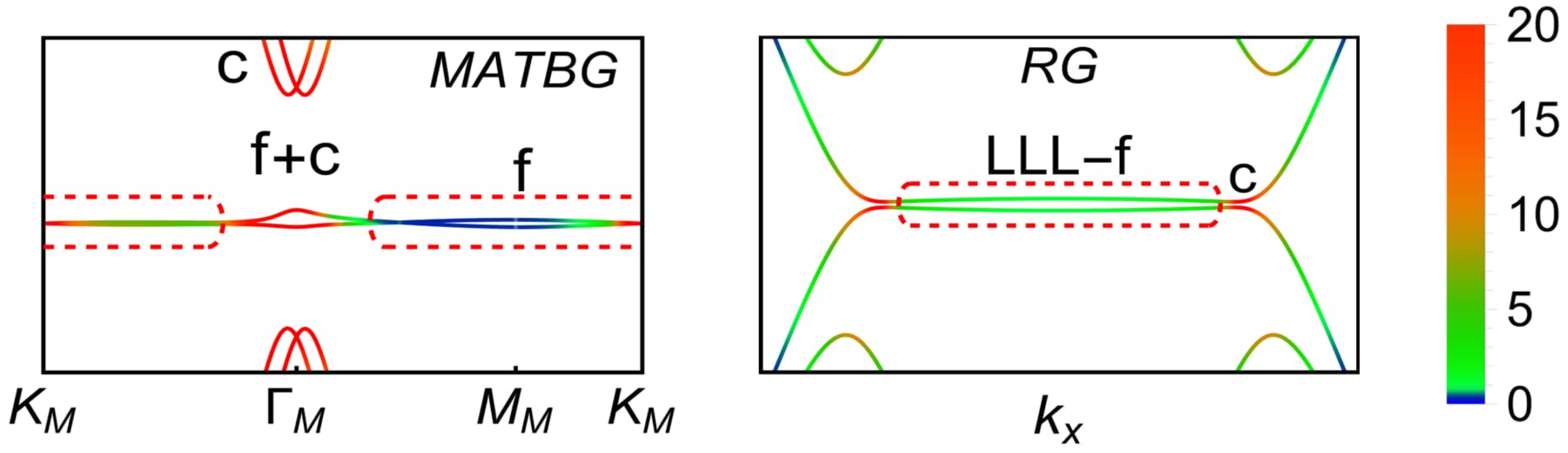

Are there other examples of unusual HFs in condensed matter?

Summary

- RG surface bands have similar QGT to LLL

- Unusual HFs localized in reduced dimensions

- Implications for other correlated phases (fractional topological phases, etc.?)

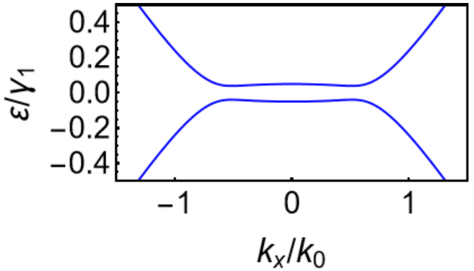

$$\frac{1}{(1-k^2)^2}\begin{pmatrix} 1 & \pm i \\ \mp i & 1 \end{pmatrix}$$

Contents

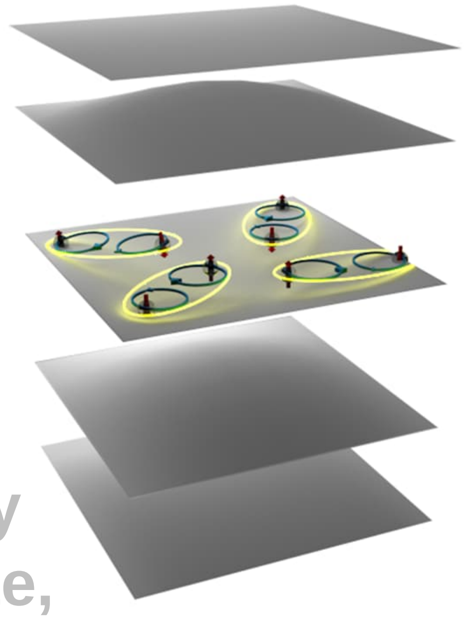

Quantum geometry and superconductivity

Lowest-Landau-level (LLL) quantum geometry of the surface states of rhombohedral graphite, and superconductivity

High topological charge lasing in a quasicrystal

Plasmonic lattices

Surface lattice resonances (SLRs)

Dispersive energy bands with polarization dependent properties

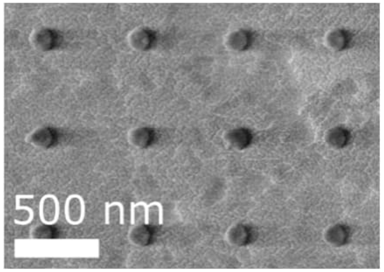

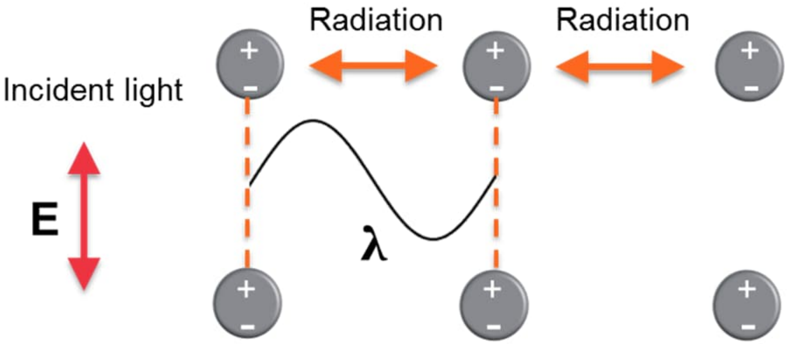

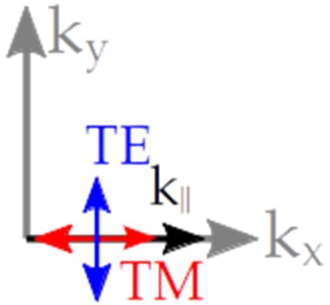

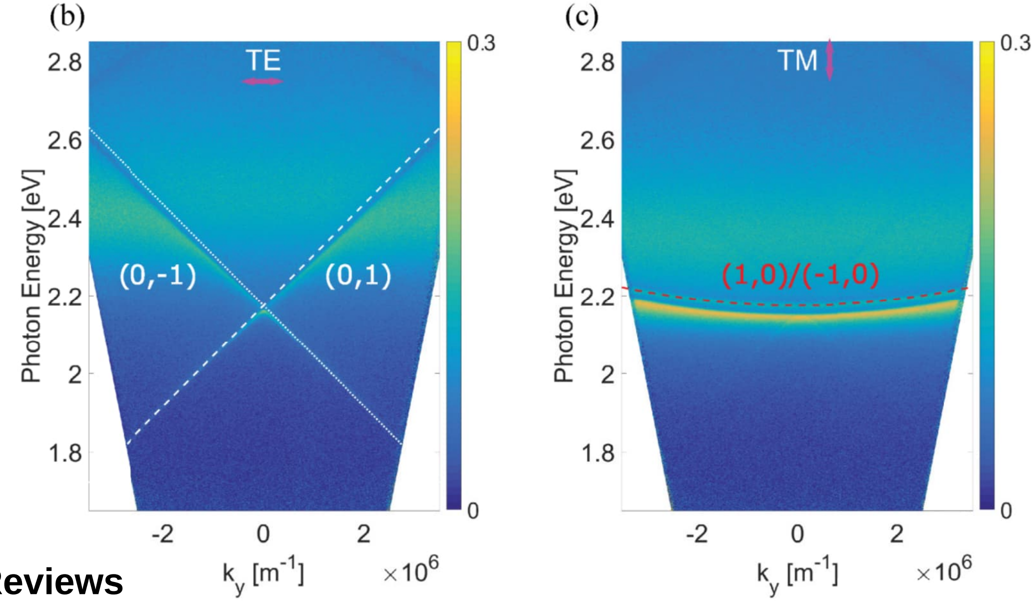

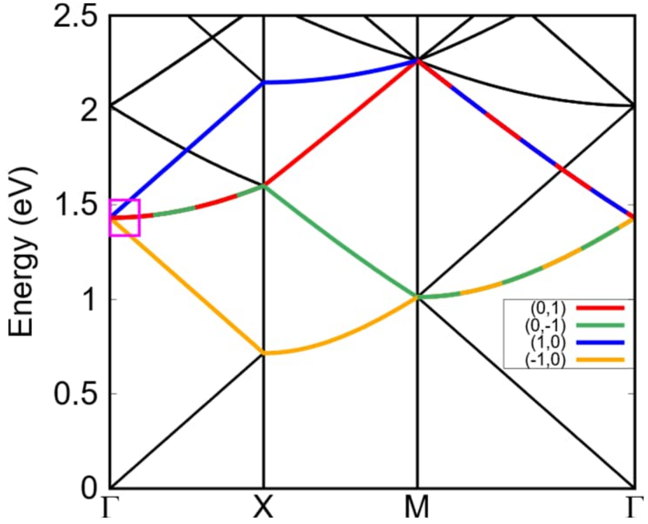

Reviews

Garcia de Abajo, Rev. Mod. Phys. 2007

Wang, Ramezani, Väkeväinen, PT, Gomez-Rivas, Odom, Materials Today 2018

Kravets, Kabashin, Barnes, Grigorenko, Chemical Reviews 2018

Our previous work: strong coupling, lasing, Bose-Einstein condensation in a plasmonic lattice, e.g.

Hakala, Moilanen, Väkeväinen, Guo, Martikainen, Daskalakis, Rekola, Julku, PT, Nature Physics 2018

Väkeväinen, Moilanen, Necada, Hakala, Daskalakis, PT, Nature Communications 2020

Moilanen, Daskalakis, Taskinen, PT, PRL 2021

Taskinen, Kliuiev, Moilanen, PT, Nano Letters 2021

Now

- **High topological charge lasing in a quasicrystal**

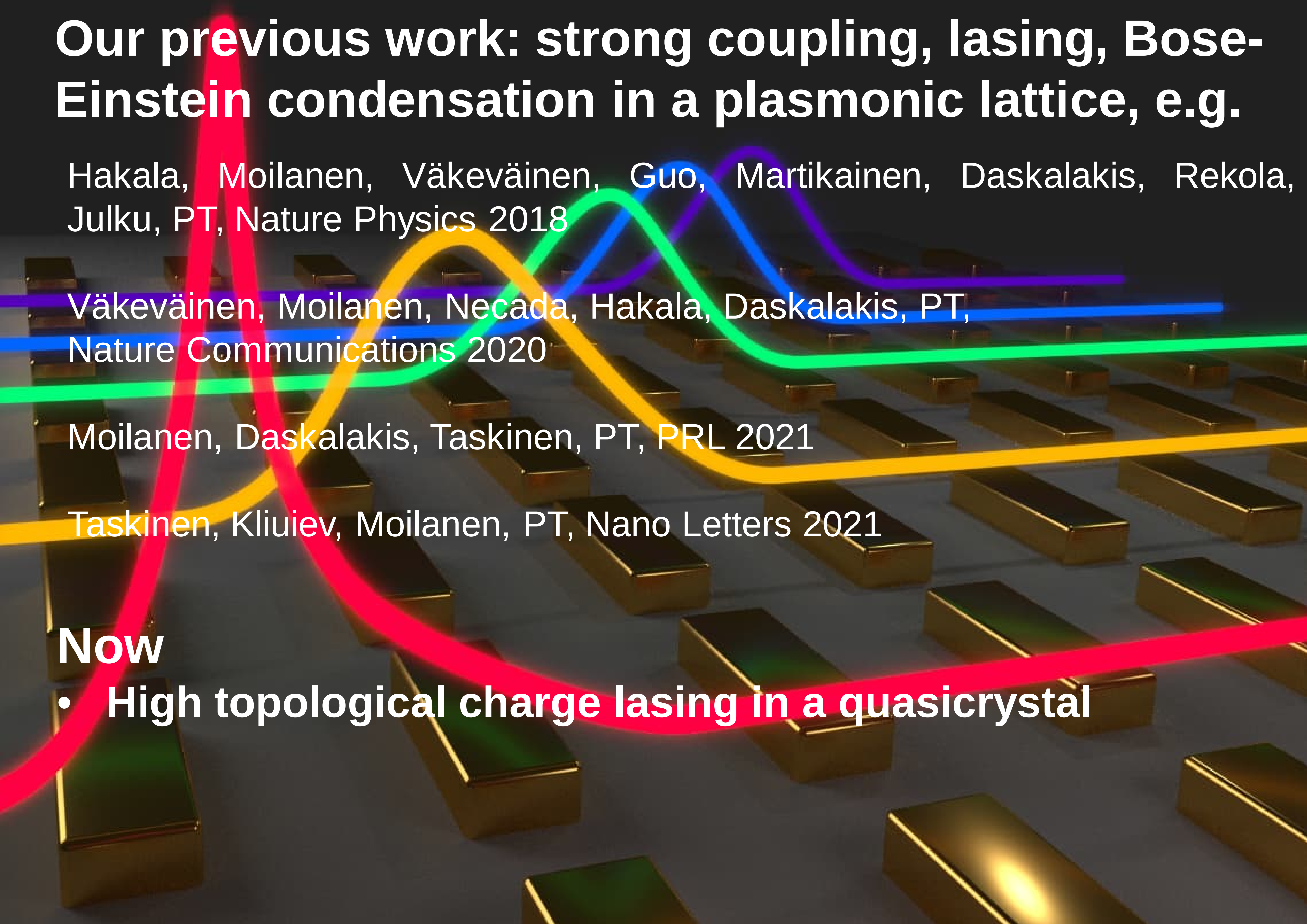

High-topological charge lasing in quasicrystals

Arjas, Taskinen, Heilmann, Salerno, PT,
Nature Communications 15, 9544 (2024)

Kristian Arjas

Jani Taskinen

Rebecca Heilmann

Grazia Salerno

Topological BICs are polarization vortices

Zhen… Soljačić*, Phys. Rev. Lett.* **113**, 257401 (2014)

Hsu… Joannopoulos, Soljačić, *Nat Rev Mater* **1,** 16048 (2016)

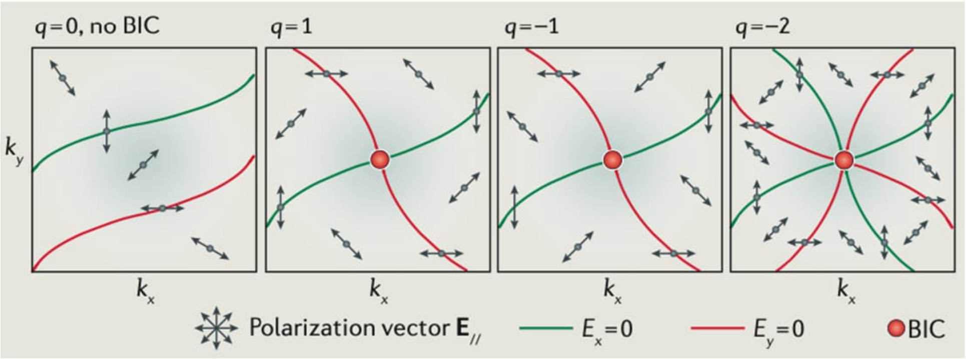

Topological BICs (bound state in continuum) cannot radiate because **there is no way to assign a far-field polarization** that is consistent with neighbouring k points.

Robust BICs are possible when there is vorticity in the polarization field, protected by the existence of a non-trivial topological invariant, the vortex charge:

$$q = \frac{1}{2\pi} \int \mathrm{d}\mathbf{k} \cdot \nabla_{\mathbf{k}} \phi(\mathbf{k})$$

$$\Phi(\mathbf{k}) = \arg[\mathbf{p}(\mathbf{k}) \cdot \hat{x} + i\mathbf{p}(\mathbf{k}) \cdot \hat{y}]$$

$$\mathbf{p}(\mathbf{k}) = (\hat{x} \cdot \langle \mathbf{u_k}(\mathbf{r}, z) \rangle)\hat{x} + (\hat{y} \cdot \langle \mathbf{u_k}(\mathbf{r}, z) \rangle)\hat{y}$$

- High-Q BICs support lasing
- They offer vector vortex beams with a topological charge and can be used for creating beams of optical angular momentum

Rybin and Kivshar, *Nature* **541**, 164 (2017)
Kodigala… Kante, *Nature* **541**, 196 (2017)
Ha… Kutznetsov*, Nat. Nanotechnol.* **13**, 1042 (2018)
Huang… Ge, Kivshar, Song, *Science* **367**, 1018 (2020)
Wang… Shi, Zi*, Nat. Phot.* **14**, 623 (2020)
Wu, Kang, Werner*, New J. Phys.* **24**, 033002 (2022)
Kang… Werner*, Adv. Optical Mater.* **10**, 2101497 (2022)

Measuring the BIC charge from lasing

$|q|$ = “Number of blobs”/2
sgn(q) from rotation: clockwise (+), anti-clockwise (-)

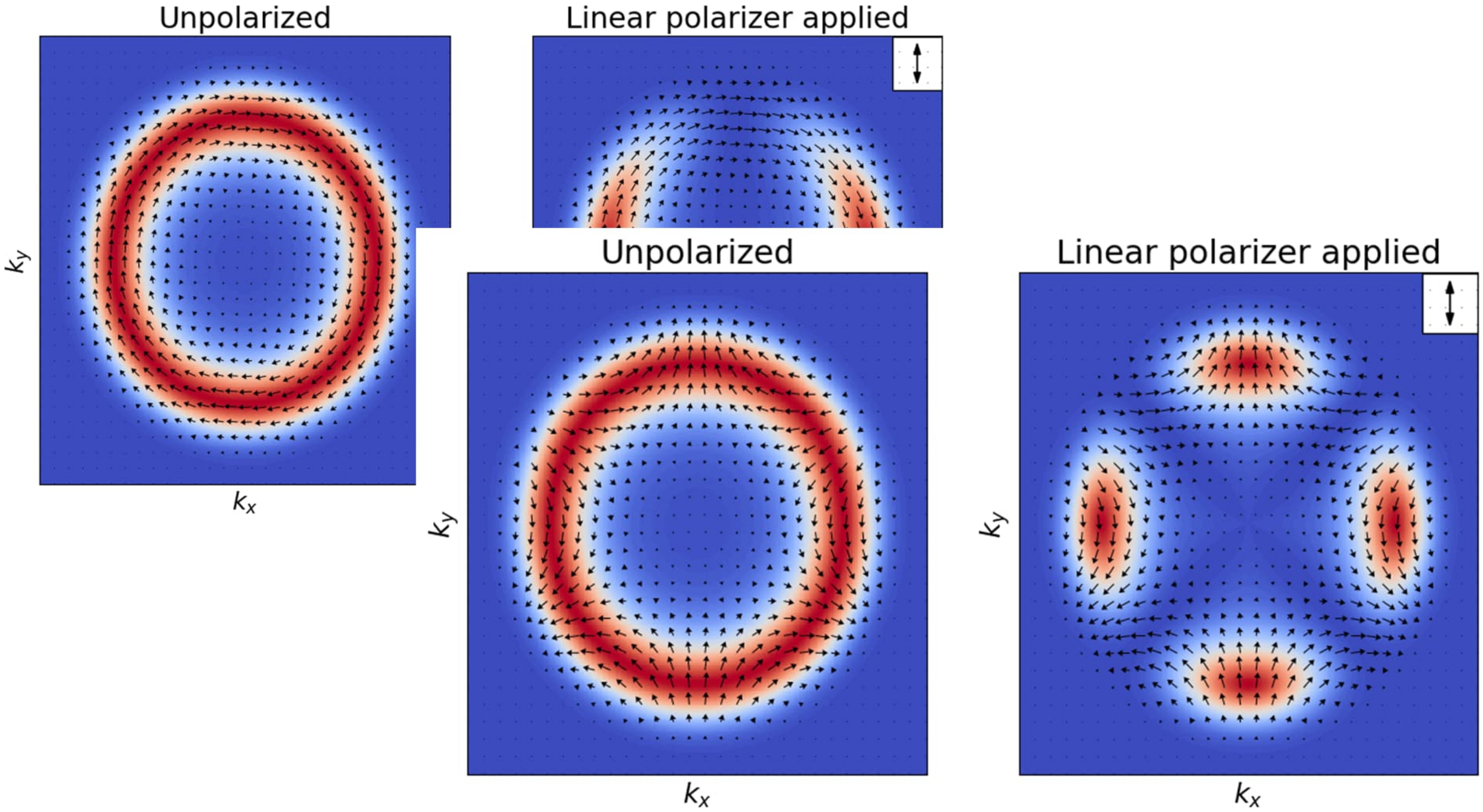

Rotational symmetries and irreducible representations

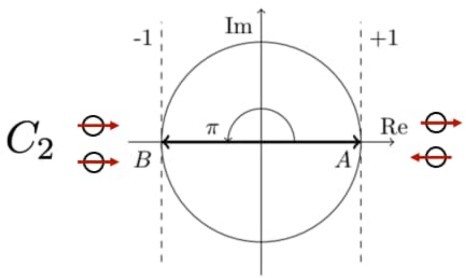

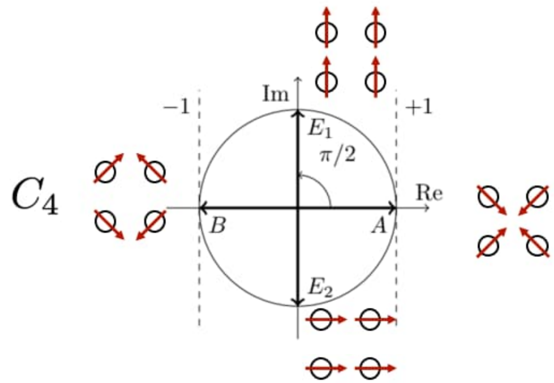

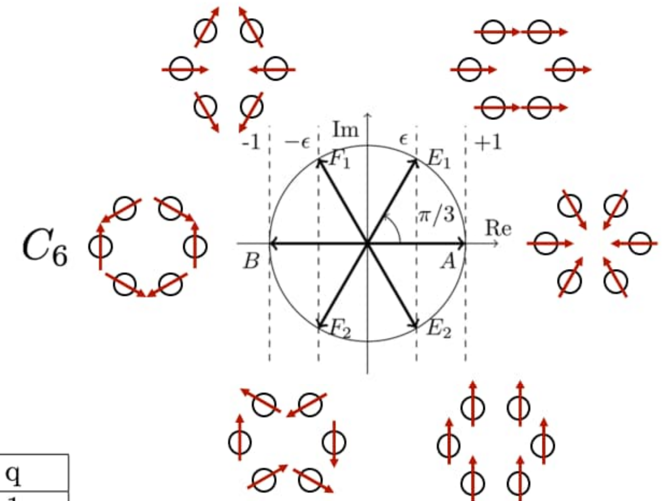

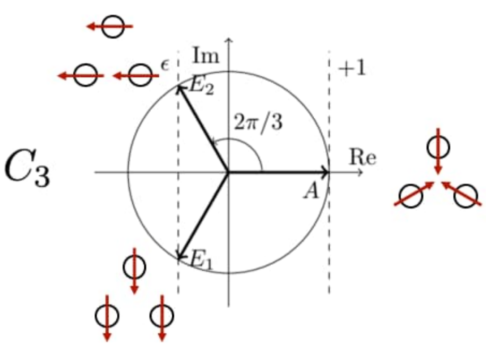

Symmetry	IR	$\arg(\epsilon_{\mathrm{IR}})$	q
C_2	A	0	+1
	B	π	0
C_3	A	0	+1
	E^*	$2\pi/3$	0
C_4	A	0	+1
	B	π	-1
	E^*	$\pi/2$	0
C_6	A	0	+1
	B	π	-2
	E_1^*	$\pi/3$	0
	E_2^*	$2\pi/3$	-1

$$q_{\mathrm{irrep}} = 1 - \frac{n}{2\pi}\arg(\epsilon_{\mathrm{irrep}})$$

Salerno, Heilmann, Arjas, Aronen, Martikainen, PT, PRL 2022

High topological charges by quasicrystals

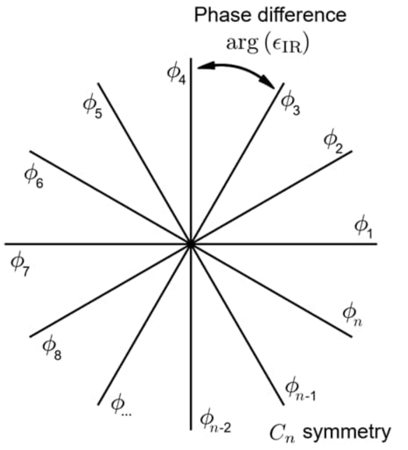

Goal

Design a lattice capable of hosting a BIC with high charge (|q| > 2)

$$q_{\mathrm{IR}} = 1 - \frac{n}{2\pi} \arg\left(\epsilon_{\mathrm{IR}}\right) + n \cdot m$$

$$m \in \mathbb{Z}$$

Design idea

1. Generate electric field interference pattern with desired symmetries
   - Near field and far-field should have same symmetry properties

2. Minimize losses in the desired mode by placing particles
   - Targeted mode has lowest losses: highest quality factor

Step 1: Empty-lattice Interference pattern

Energy density $$\rho_{IR}(\mathbf{r}) = \left|\sum_j \mathbf{E}_{IR,j}(\mathbf{k}_j, \mathbf{r})\right|^2 = \left|\sum_j e^{i\mathbf{k}_j\cdot\mathbf{r}} \begin{bmatrix} a_{IR,j} \\ b_{IR,j} \end{bmatrix}\right|^2$$

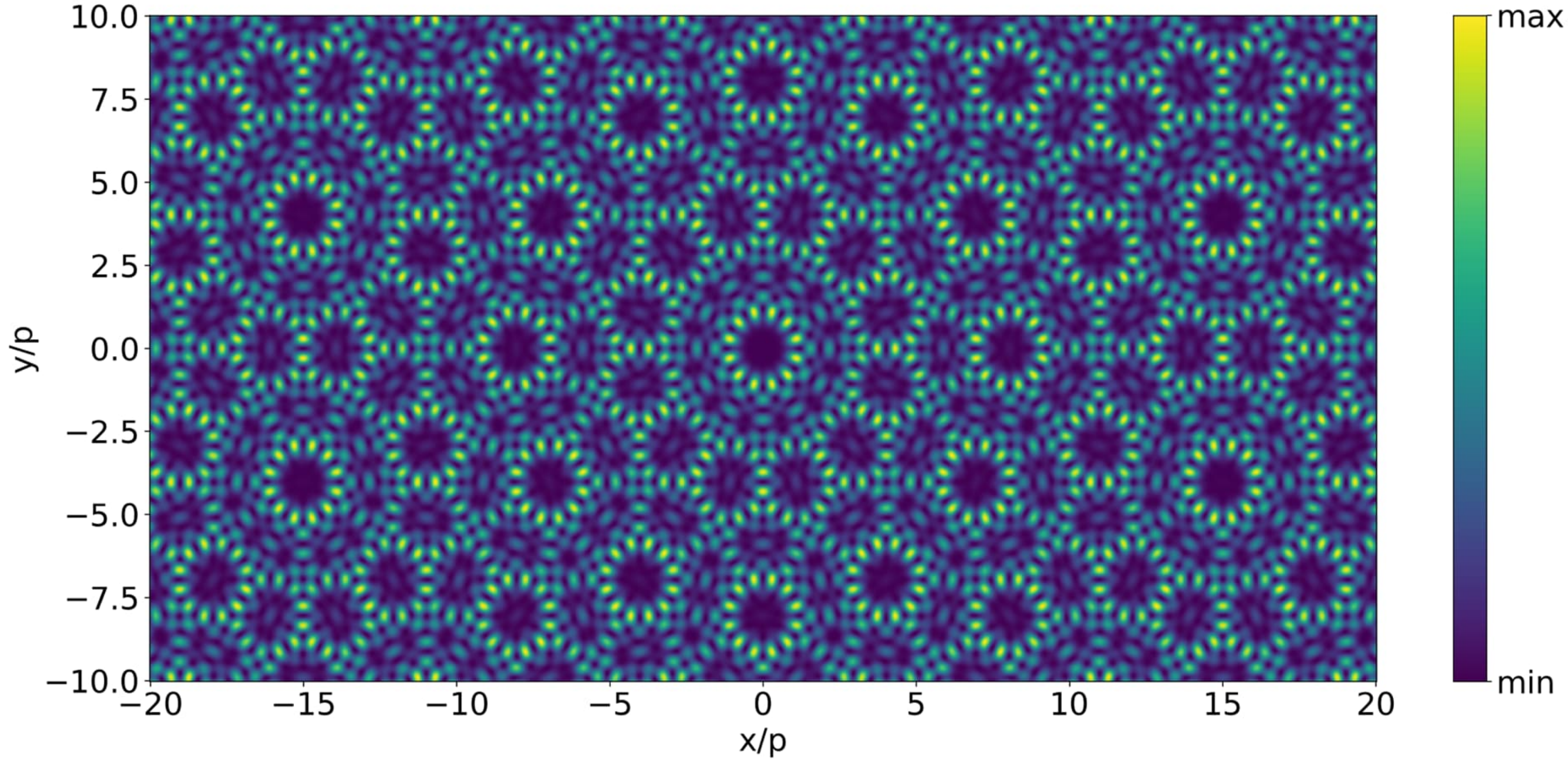

Interference pattern for IR *B*

Step 2: Moiré-scheme

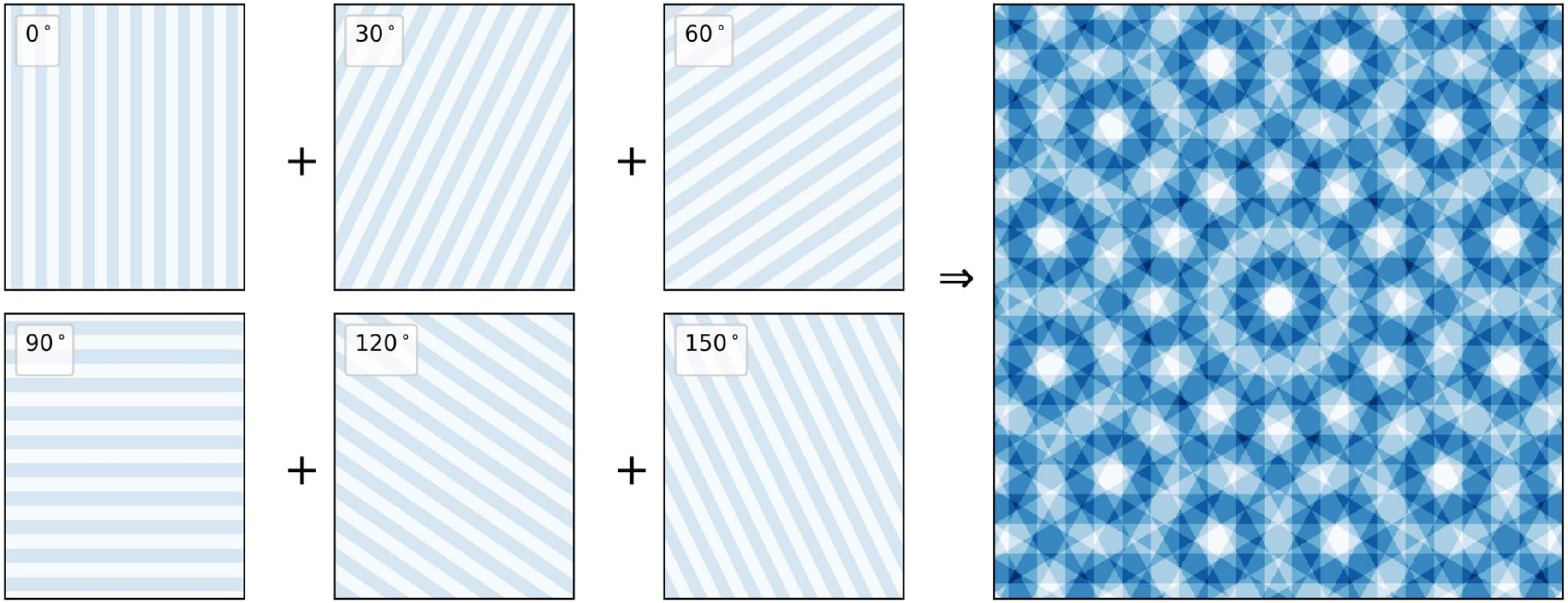

Particles placed in the shaded regions are roughly periodic in given direction. Selecting particles in darker regions allows us to find the particles that best fit with the desired diffracted orders.

Step 3: Density Equalization

C_{12}-sample SEM image

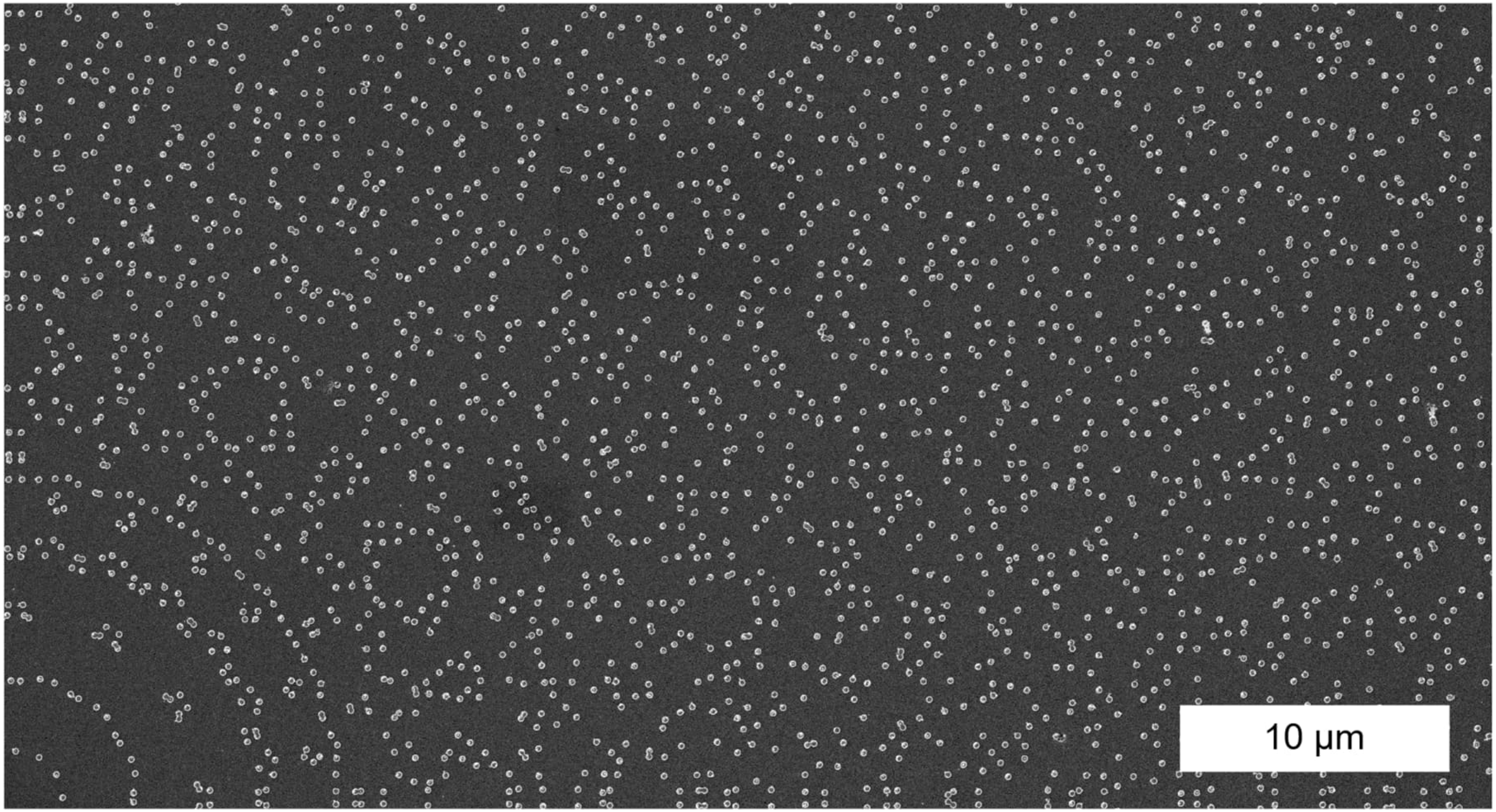

~3% of the total sample area

Measurements

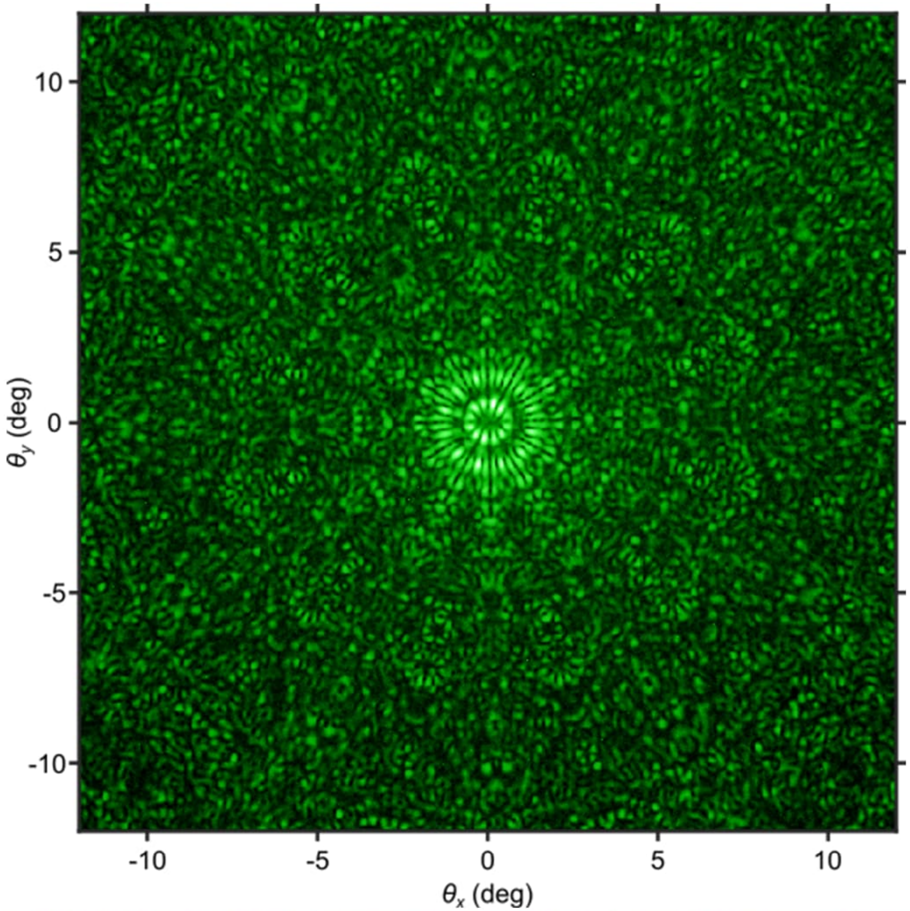

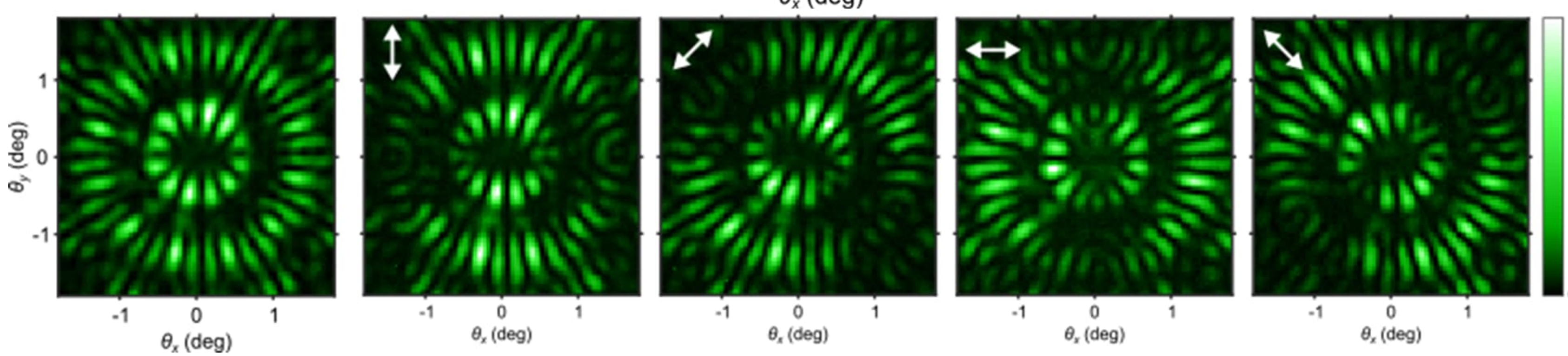

Two charges nearby

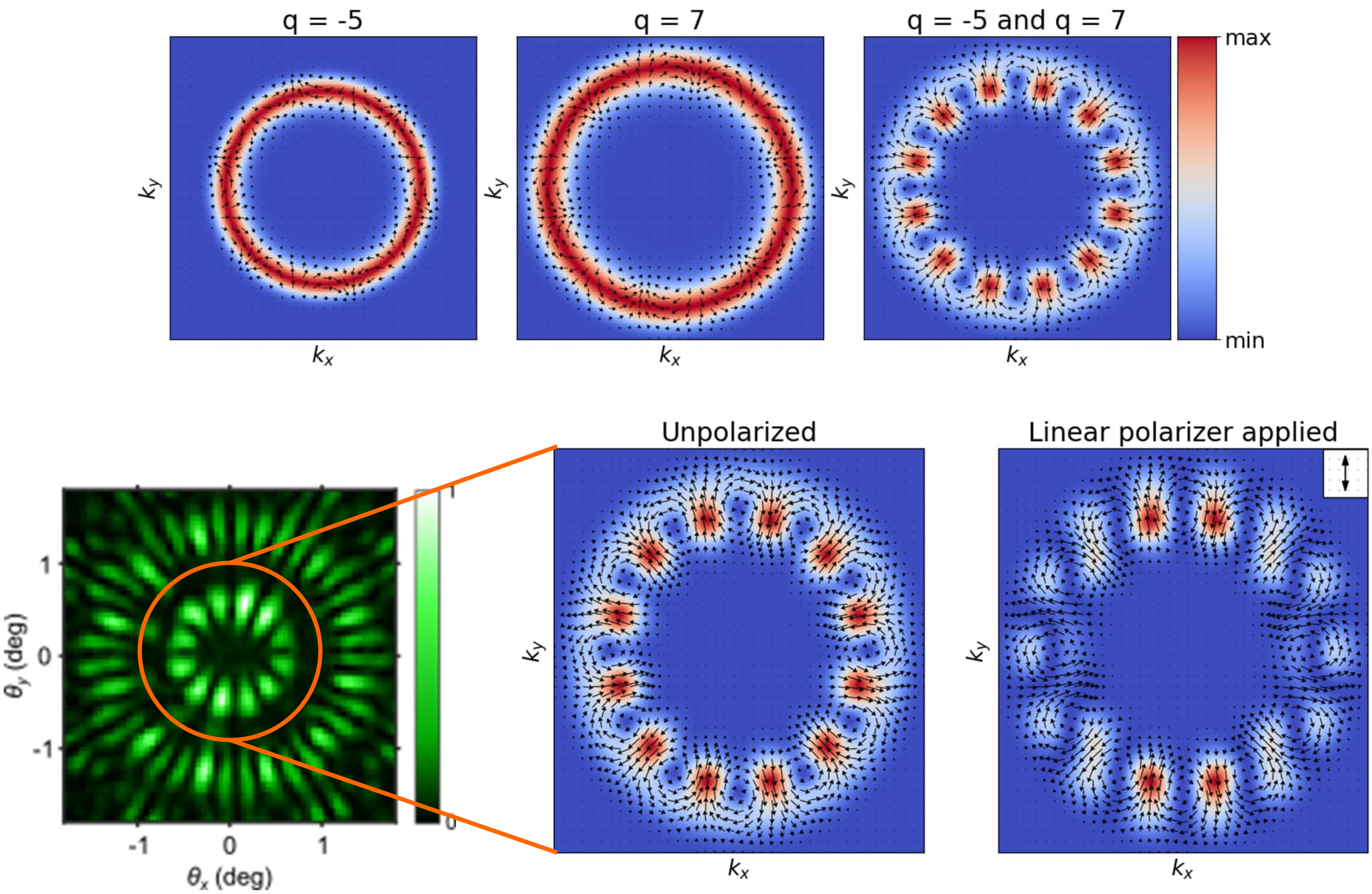

Polarization resolved measurements

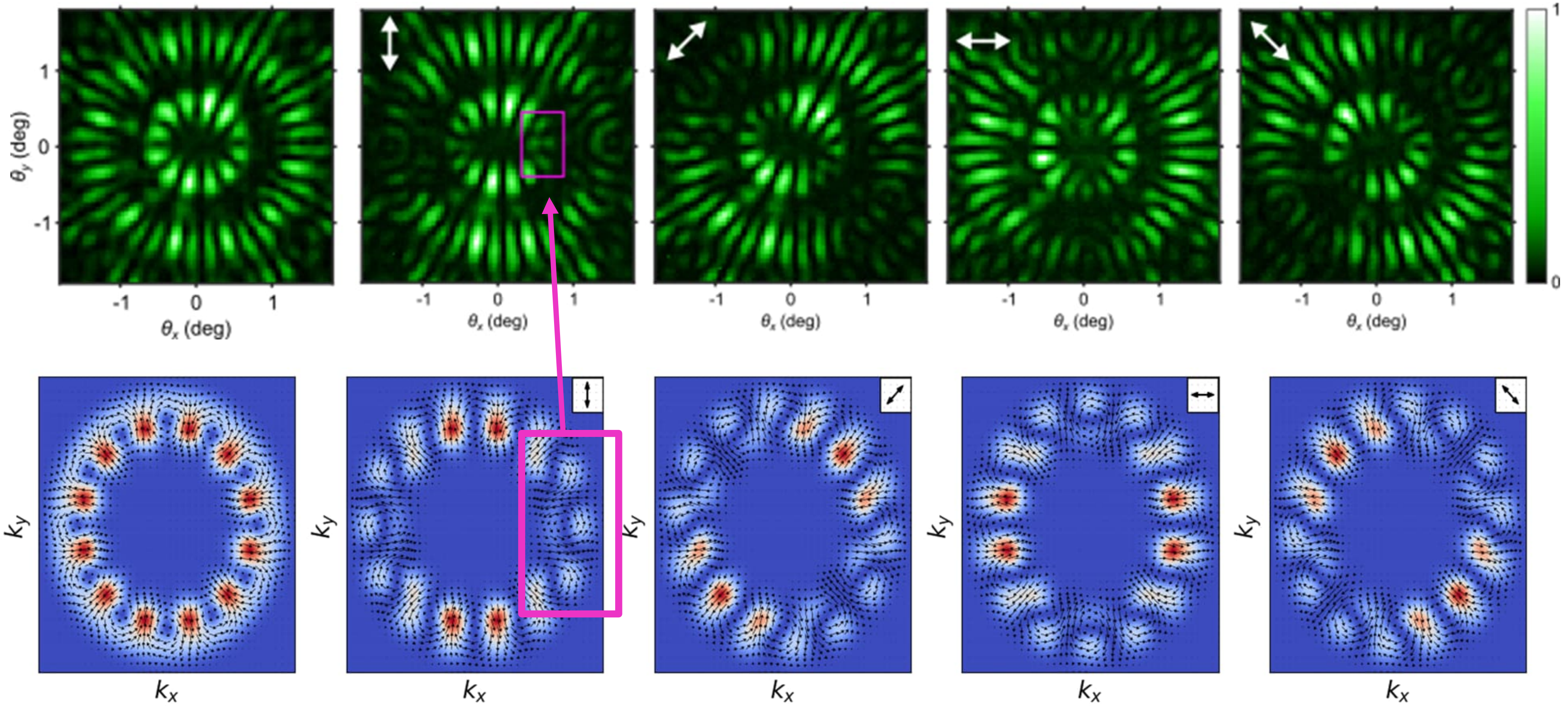

Topological charges up to +19!

$$q_{\mathrm{IR}} = 1 - \frac{n}{2\pi}\arg\left(\epsilon_{\mathrm{IR}}\right) + n \cdot m \quad m \in \mathbb{Z}$$

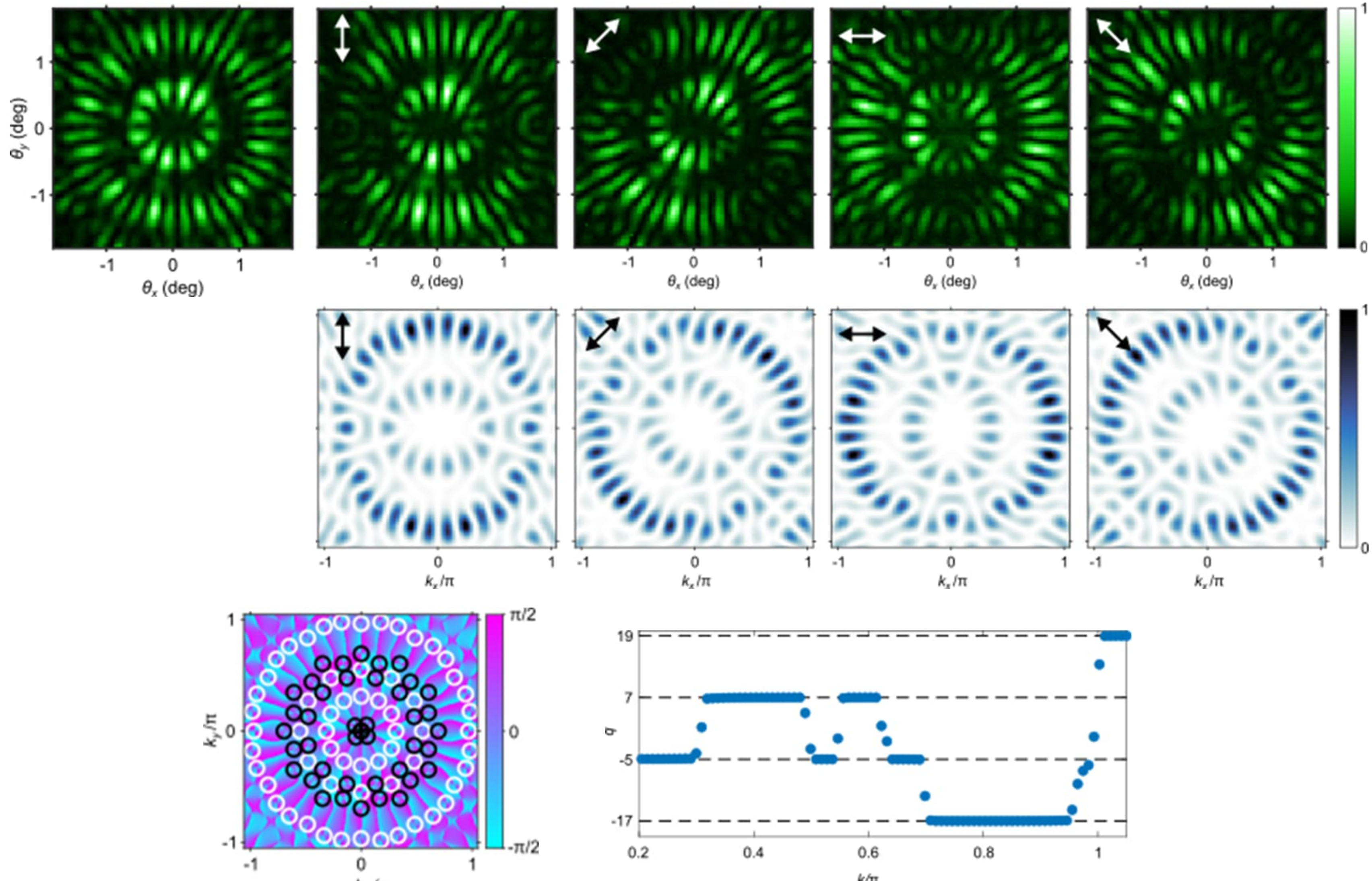

Why primes (-5, +7, -17, +19, …)?

$$q_{\mathrm{IR}} = 1 - \frac{n}{2\pi}\arg\left(\epsilon_{\mathrm{IR}}\right) + n \cdot m \qquad m \in \mathbb{Z}$$

For n=12, and the irrep character π, we have
q = 1 + 6 (m-1) = 1 + 6 n’

Dirichlet’s theorem: for any co-primes a and d, the are infinitely many primes of the form
q = a + d n’

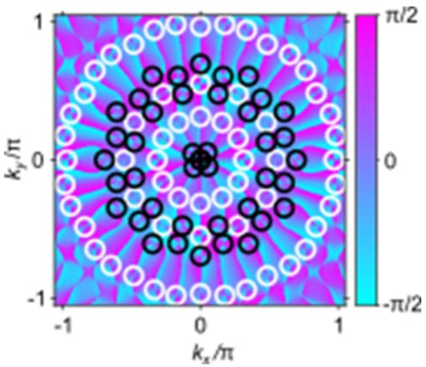

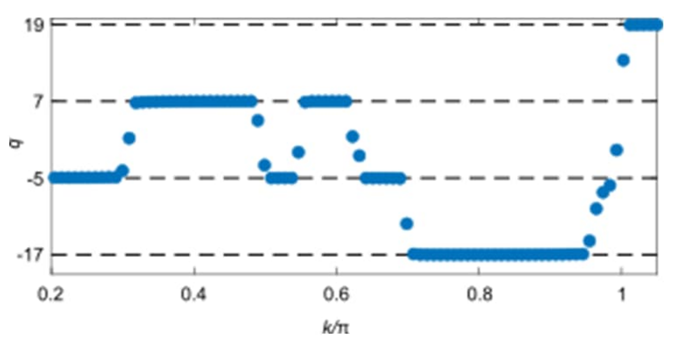

Flat-band-like emission

Lasing

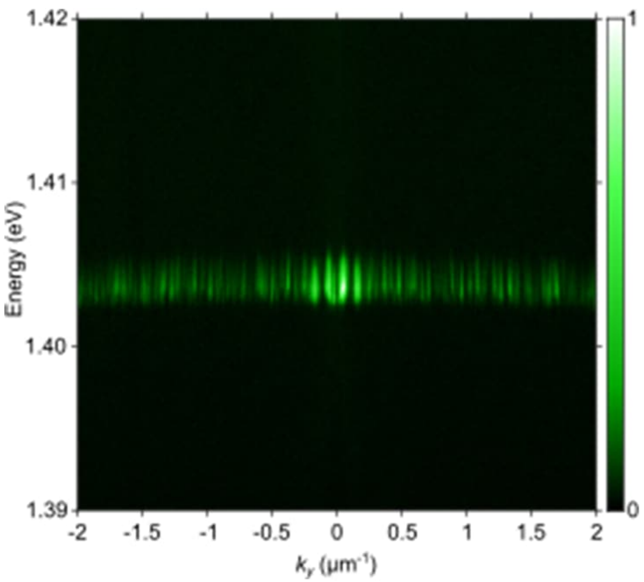

Dispersions without lasing

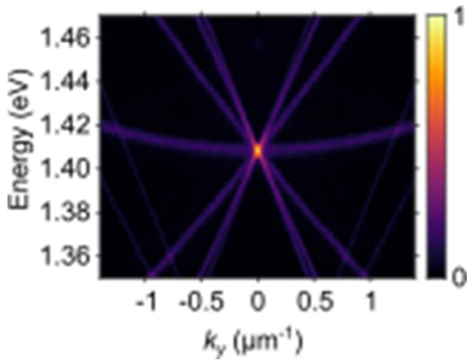

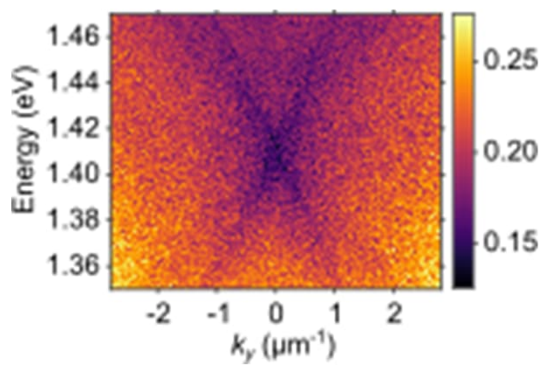

Quasicrystals have a continuum of Bragg peaks

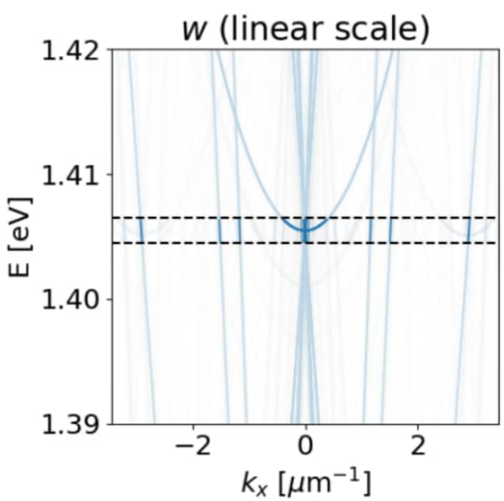

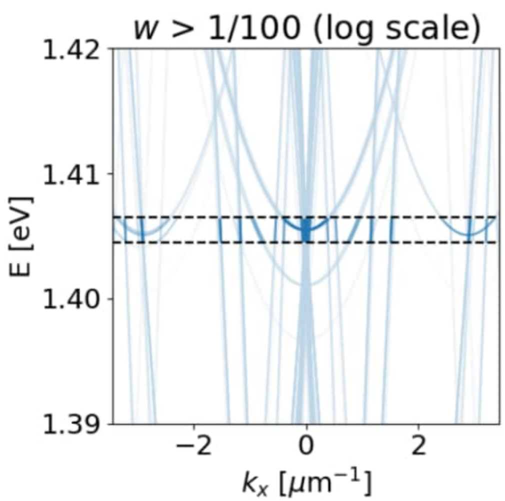

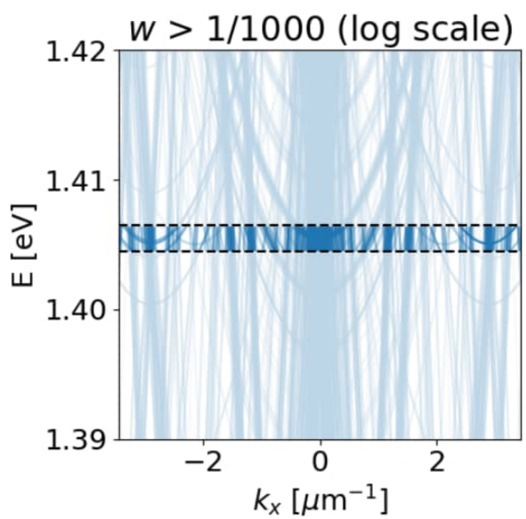

Summary

Quantum geometry allows flat band superconductivity

Rhombohedral graphite: LLL quantum geometry of surface states

Lasing with unprecedentedly high topological charges:
-5, +7, -17 and +19!
Novel quasicrystal design
Flat-band like lasing

Outlook

Superconductivity at high temperatures

Interplay of quantum geometry and topology with interactions and gain

Exploiting quasicrystals for beam design,
Transfer of the concept to other systems/materials